



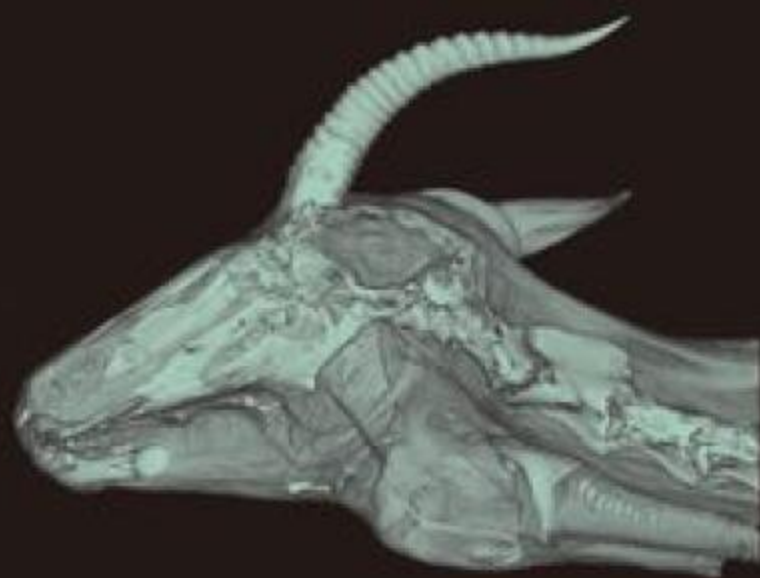
H. Endo · R. Frey
Editors



Anatomical

Imaging

Towards a New Morphology



 Springer

6

Using CT to Peer into the Past: 3D Visualization of the Brain and Ear Regions of Birds, Crocodiles, and Nonavian Dinosaurs

Lawrence M. Witmer¹, Ryan C. Ridgely¹, David L. Dufeu², and Molly C. Semones³

6.1 Introduction

Until relatively recently, information on the internal skull structures of fossil taxa relied on fortuitous breaks, aggressive removal of rock matrix (Galton 1989, 2001), sectioning with a saw (Osborn 1912), or serial ground thin-sectioning (Stensiö 1963), all of which potentially risk damage to the fossil specimen (or even consume it entirely in the case of ground thin-sections). In some cases, casts of internal structures, such as the brain cavity and labyrinth of the inner ear, were preserved as ‘natural endocasts’ by infilling with more resistant matrix (e.g., Newton 1888). In most cases, however, physical endocasts are made after matrix removal by coating internal cavities with latex and then removing the cured replica, referred to as a latex endocast (Radinsky 1968; Jerison 1973; Hopson 1979). The process of making latex endocasts poses further risks to the fossil, and for many fragile specimens, such an approach has been unfeasible.

The advent of non-invasive, non-destructive radiological approaches – specifically, X-ray computed tomography, better known as CT or CAT scanning – has revolutionized the study of fossil specimens (Conroy and Vannier 1984; Carlson et al. 2003), allowing the investigator to see through the bone and rock matrix and visualize internal structures. Moreover, CT scanning is an effective 3D digitizing tool, mapping all points within the

subject into x-y-z coordinate space. This property allows features of interest (such as the brain cavity, inner ear, neurovascular canals, air sinuses, etc.) to be digitally highlighted and extracted for visualization and quantification (e.g., Sampson and Witmer 2007). In particular, CT scanning has rejuvenated the subject of ‘paleoneurology,’ the study of brain evolution in the fossil record. Paleoneurology previously relied exclusively on physical (natural or latex) endocasts (Jerison 1973; Edinger 1975; Hopson 1979; Hurlburt 1996; Buchholtz and Seyfarth 1999; Wharton 2002). Recent years, however, have witnessed an explosion of CT-based studies of the brain cavity (and sometimes also the labyrinth) in a range of vertebrates (Rogers 1998, 1999, 2005; Brochu 2000, 2003; Larsson 2001; Marino et al. 2003; Domínguez Alonso et al. 2004; Franzosa 2004; Franzosa and Rowe 2005; Maisey 2005; Kurochkin et al. 2006; Macrini et al. 2006; Kundrát 2007).

We present some results here of our large CT-based project on the evolution of the brain and ear regions of archosaurs (Witmer et al. 2003; Holliday et al. 2006; Sampson and Witmer 2007; Witmer and Ridgely, in press; Hurlburt et al. in press). Archosaurs are the group of animals that includes birds and crocodylians today and in the Mesozoic Era included nonavian dinosaurs, pterosaurs, and a variety of early forms. The project has sampled taxa from throughout Archosauriformes, generating to date about 150 CT datasets of extinct

¹Department of Biomedical Sciences and College of Osteopathic Medicine, ²Department of Biological Sciences, ³Honors Tutorial College, Ohio University, Athens, Ohio 45701 USA

taxa. Moreover, there has likewise been an extensive sampling of extant taxa, and not just archosaurs, but also the extant outgroups of archosaurs (lepidosaurs, turtles, and mammals). This study is framed within the extant phylogenetic bracket approach (Witmer 1995) whereby the extant outgroups (e.g., birds, crocodilians, lizards) of the fossil taxon of interest (e.g., dinosaurs) provide critical information on the causal associations between soft tissues and their osteological correlates. That is, the extant taxa and their still-present soft tissues provide essential guides to the significance of particular bony details, which can then be directly compared with the bony structures of the fossil specimens. Thus, although the study presented here focuses on certain dinosaur taxa, the extant taxa (Australian freshwater crocodiles and great horned owls) provide the necessary ground-truthing to interpret and infer the soft-tissue structures of dinosaurs (Fig. 6.1).

The dinosaurs we present here include two members of the long-necked sauropod clade, *Camarasaurus lentus* and *Diplodocus longus*. These two sauropods not only allow comparison of variation in brain and ear structure within a group of dinosaurs, but also demonstrate differences in head orientation as indicated by labyrinth orientation (Witmer et al. 2003). Sauropod brain and ear structure will then be compared to that of the gigantic predatory theropod dinosaur *Tyrannosaurus rex* to provide some insight into the sensorineural differences between carnivorous and herbivorous dinosaurs. Rather than provide elaborate anatomical descriptions in the text, we will draw on the benefits of advanced 3D visualization, and let our illustrations ‘do the talking.’ The text will emphasize comparison and interpretation.

Institutional abbreviations – AMNH, American Museum of Natural History, New York City,

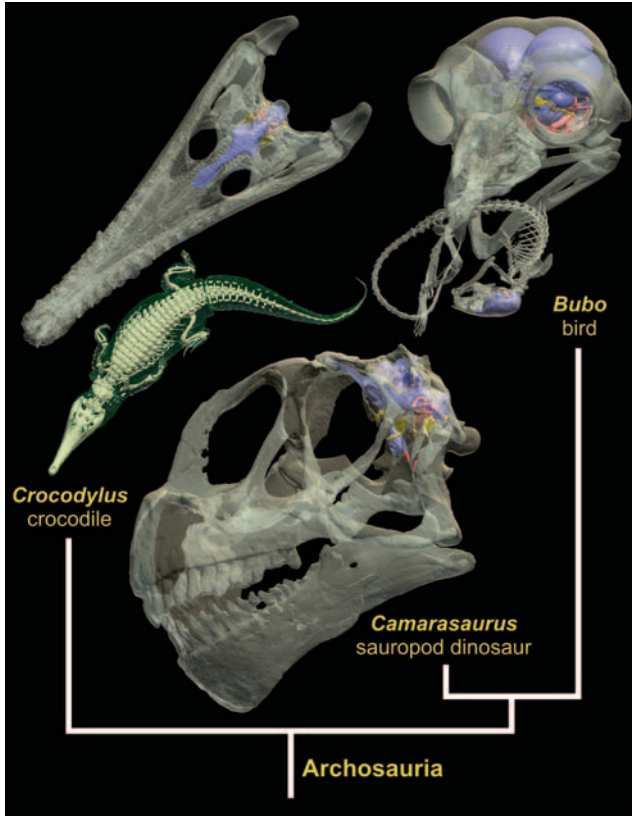


FIG. 6.1. The extant phylogenetic bracket (Witmer 1995) of nonavian dinosaurs, as exemplified by the sauropod dinosaur *Camarasaurus lentus* (CM 11338, in left lateral view). The extant outgroups of the fossil taxa provide information on attributes such as soft-tissue morphology and behavior that are not preserved in the fossils. The extant outgroups of nonavian dinosaurs are crocodilians (as exemplified by *Crocodylus johnstoni*, OUV 10425, in dorsal view) and birds (as exemplified by *Bubo virginianus*, OUV 10220, in left rostralateral view with *Mus musculus* [OUV 10449] in its jaws). The images are surfaces renderings of CT scan data, with the skull rendered semitransparent revealing the cranial endocast (in blue) and other structures (see Color Plates, Fig. 6.1).

New York; ANSP, Academy of Natural Sciences, Philadelphia, Pennsylvania; CM, Carnegie Museum of Natural History, Pittsburgh, Pennsylvania; HMS, Houston Museum of Natural Science, Houston, Texas; ISIR, Indian Statistical Institute, Calcutta, India; OUVC, Ohio University Vertebrate Collections, Athens, Ohio.

Anatomical Abbreviations – as, articular sinus; bsr, basisphenoid recess(es); c, cochlea; car, cerebral carotid artery canal; cbl, cerebellum; cer, cerebral hemisphere; col, columella (= stapes); crc, crus communis; csc, caudal (posterior vertical) semicircular canal; csca, ampulla of caudal semicircular canal; ctp, cavum tympanicum proprium; ctr, caudal tympanic recess; cvcm, caudal middle cerebral vein; de, dural expansion; dp, dural peak; dls, dorsal longitudinal sinus; dtr, dorsal tympanic recess; dv, diploic vein draining bone tissue; ed, endolymphatic duct; ev, ethmoid vein; fc, fenestra cochleae (= round window); fl, flocculus (= cerebellar auricle); fp, foramen perilymphaticum (sauropods); fv, fenestra vestibuli (= oval window); h, hyperpallium (= Wulst, eminentia sagittalis); itr, intertympanic recess; lab, endosseous labyrinth; lsc, lateral (horizontal) semicircular canal; lsca, ampulla of lateral semicircular canal; lscr, lateral subcondylar recess; mpr, median pharyngeal recess; mscr, medial subcondylar recess; ob, olfactory bulb; ocv, orbitocerebral vein; oevc, orbital emissary vein canal; opt, optic tectum (= lobe); ovs, occipital venous sinus; pfo, pituitary (= hypophyseal) fossa; pin, pineal peak; po, pons; ptr, pharyngotympanic (= Eustachian) recess; qs, quadrate sinus; rde, rostral dural expansion; rsc, rostral (anterior vertical) semicircular canal; rsca, ampulla of rostral semicircular canal; rtr, rostral tympanic recess; rvcm, rostral middle cerebral vein; s, siphonium; sin, blind dural venous sinus of hindbrain; sps, sphenoparietal sinus; ssr, subsellar recess; st, stapedia artery; ts, transverse sinus; tvn, tuber ventromediale of the cerebrum; vc, venous canal; vcd, dorsal head vein; ve, vestibule of inner ear; vls, ventral longitudinal sinus; vt, vallecule telencephali; I, olfactory canal; II, optic nerve canal; III, oculomotor nerve canal; IV, trochlear nerve canal; V₁, ophthalmic nerve canal; V₂, maxillary nerve canal; V₂₋₃, maxillomandibular nerve canal; V₂₋₃/VII, common external opening in braincase for maxillomandibular and facial nerve canals; V_{2-so}, canal for supraorbital branch of maxillary nerve; V₃, mandibular nerve canal; V_{gang}, trigemi-

nal (Gasserian) ganglion; V_{tym}, tympanic branch of trigeminal nerve canal; VI, abducens nerve canal; VII, facial nerve canal; VII_h, canal for hyomandibular ramus of facial nerve; VII_{pal}, canal for palatine ramus of facial nerve; IX, glossopharyngeal nerve canal; IX–XI, shared canal for glossopharyngeal, vagus, and accessory nerves and accompanying vessels; X, vagal nerve canal; X_{tym}, canal for tympanic branch of glossopharyngeal and vagus nerves; XII, hypoglossal nerve canal.

6.2 Materials

As noted above, the broader sample of extinct archosaurs and extant amniotes that have been analyzed includes many dozens of taxa. The extant archosaur taxa presented here are the following: (1) Crocodylia, Crocodylidae, *Crocodylus johnstoni* (Australian freshwater crocodile; OUVC 10425, an intact frozen carcass of an adult captive individual); and (2) Aves, Strigiformes, Strigidae, *Bubo virginianus* (great horned owl; OUVC 10220, a dried skull of an adult wild individual). The fossil dinosaur taxa presented here are the following: (1) Dinosauria, Saurischia, Sauropodomorpha, Macronaria, *Camarasaurus lentus* (CM 11338, a nearly complete skull of a juvenile individual); (2) Dinosauria, Saurischia, Sauropodomorpha, Diplodocoidea, *Diplodocus longus* (CM 11161, a nearly complete skull of an adult individual; CM 3452, a nearly complete skull of a subadult individual; AMNH 694, a sagittally sectioned braincase of a subadult individual); and (3) Dinosauria, Saurischia, Theropoda, Coelurosauria, *Tyrannosaurus rex* (AMNH 5117, a braincase of a subadult individual). Additional specimens of *T. rex* and other tyrannosaurids also were studied in connection with other projects (see Witmer and Ridgely in press for details). All of the sauropod specimens were collected from the Late Jurassic Morrison Formation; CM 11338, 11161, and 3452 come from Dinosaur National Monument, Utah, and AMNH 694 comes from Bone Cabin Quarry, Wyoming. AMNH 5117 was collected from the Late Cretaceous Lance Formation of Converse County, Wyoming. Figure 6.2 presents a cladogram depicting the relationships of these five focal taxa.

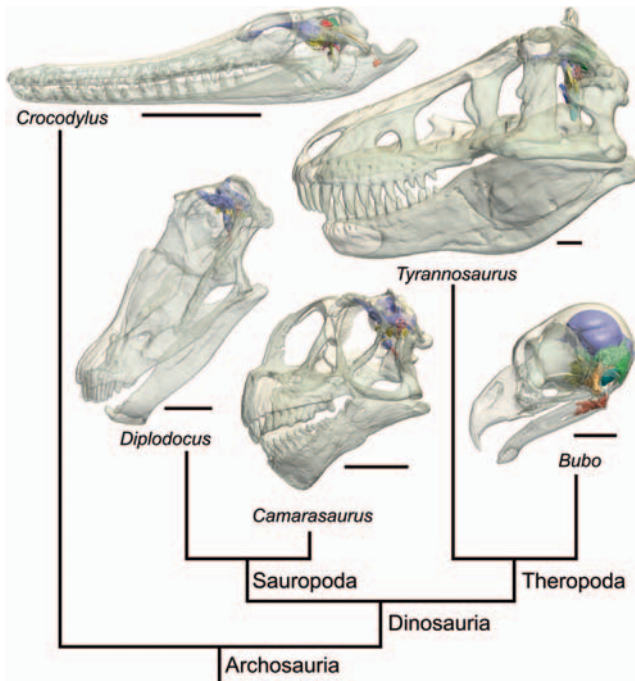


FIG. 6.2. Diagram of the phylogenetic relationships of the principal taxa discussed in the text. From left, the extant crocodylian *Crocodylus johnstoni* (OUVC 10425), the diplodocoid sauropod *Diplodocus longus* (CM 11161), the macronarian sauropod *Camarasaurus lentus* (CM 11338), the basal coelurosaurian theropod *Tyrannosaurus rex* (AMNH 5117), and the avian theropod (bird) *Bubo virginianus* (OUVC 10220). These sauropods and theropods are saurischian dinosaurs. The images are surface renderings of CT scan data. Bony skulls are depicted as transparent, revealing such internal structures as the brain cast, labyrinth, and pneumatic sinuses. All skulls are oriented in their 'alert' postures, determined by orienting the skull such that the lateral semicircular canal is horizontal. Scale bars equal 10 cm, except that for *B. virginianus* which equals 2 cm (see Color Plates, Fig. 6.2).

6.3 Methods

CT scanning of the extant crocodile (OUVC 10425), *Camarasaurus* (CM 11338), *Diplodocus* (CM 3452), and *Tyrannosaurus* (AMNH 5117) took place at O'Bleness Memorial Hospital (OBMH) in Athens, Ohio, using a General Electric (GE) LightSpeed Ultra Multislice CT scanner. This scanner was equipped with the Extended Hounsfield option (which greatly improves resolvability of detail from dense objects such as fossils by extending the dynamic range of images as much as 16-fold) and a 'bow-tie' filter (which decreases beam-hardening artifacts). These specimens were scanned helically at a slice thickness of 625 μm , 120 kV, and 200–300 mA. The other specimens of *Diplodocus* were scanned at OBMH with a GE HiSpeed FX/i Multislice helical scanner at a slice thickness of 1 mm (AMNH 694) or 2 mm (CM 11161), 120–140 kV, and 150 mA. The raw scan data were reconstructed using a bone algorithm. Data were output from the scanners in DICOM format, and then imported into Amira 3.1.1 or 4.1.1 (Mercury-TGS, Chelmsford, MA) for viewing, analysis, and visualization.

The extant owl skull (OUVC 10220) was scanned at the Ohio University MicroCT (OU μ CT) facility

in Athens, Ohio, using a GE eXplore Locus in vivo Small Animal MicroCT Scanner. It was scanned (with a domestic mouse, *Mus musculus* [OUVC 10449], in its jaws; Fig. 6.1) at a slice thickness of 92 μm , 80 kV, 450 μA . The resulting volume data (in VFF format) were exported from MicroView 2.1.2 (open-sourcesoftware developed by GE; microview.sourceforge.net) in DICOM format, which were then subsequently imported into Amira.

Data derived from both OBMH and OU μ CT were analyzed on 32- and 64-bit PC workstations with 4 GB of RAM and nVidia Quadro FX 3000 or 4500 video cards and running Microsoft Windows XP Professional, Windows XP Professional x64, or Linux 2.6.18 (Debian 4.0 distribution). Structures of interest (e.g., cranial endocast, labyrinth, air sinuses, etc.) were highlighted and digitally extracted using Amira's segmentation tools for quantification and visualization. Both surfaces and volumes were generated, and were used to illustrate this paper. To facilitate discussion, we will refer to the digital casts of structures as if they were the structures themselves (e.g., 'lateral semicircular canal' versus 'digital cast of lateral semicircular canal'). Additional visualizations of the CT scan data are available on www.ohio.edu/WitmerLab.

6.4 Results

As noted earlier, we will rely more on illustration than text to convey anatomical form. We begin this section with a presentation of the extant taxa because the identifications of soft-tissue structures, as well as their relationships to bony structures, have been confirmed by other means (e.g., dissection). Moreover, in the case of the crocodile, an intact specimen was scanned, and many soft-tissue components can be observed in the scan data. We follow with a presentation of the fossil taxa, beginning with the two sauropods and then *Tyrannosaurus*, basing our identifications in part on the crocodile and owl presented here but also on the dozens of other extant and fossil archosaurs we have analyzed as part of the broader project.

6.5 Extant Outgroups: *Crocodylus johnstoni*, Australian Freshwater Crocodile

The cranial endocast, endosseous labyrinth, and columella of *Crocodylus johnstoni* (OUVC 10425) are depicted in Figure 6.3. The endocast resembles in many ways those generated for *C. acutus* (Colbert 1946a) and *C. moreletii* (Franzosa 2004), although this is the most detailed cranial endocast published to date for any crocodilian. As is generally the case for reptiles (Jerison 1973; Hopson 1979), the brain itself does not fill the endocranial cavity, and thus the endocast is in large measure a cast of the dural envelope. As a result, many of the brain parts are obscured by the overlying dural venous sinuses and the dura itself. For example, as

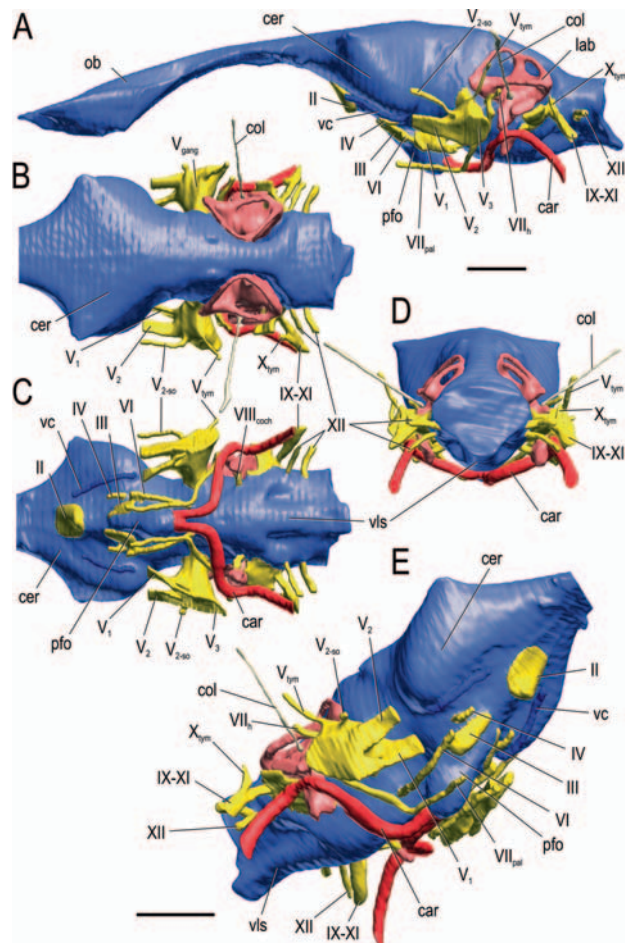


FIG. 6.3. Cranial endocast, endosseous labyrinth, and some endocranial vascular structures of an Australian freshwater crocodile, *Crocodylus johnstoni* (OUVC 10425), derived from surface renderings of CT scan data. **A**, left lateral view. **B**, dorsal view, with olfactory tract truncated. **C**, ventral view, with olfactory tract truncated. **D**, caudal view. **E**, right rostroventrolateral view. Color scheme: cranial endocast, blue; endosseous labyrinth, pink; nerve canals (most of which also transmit veins), yellow; smaller venous canals, dark blue; arterial canals, red; columella, pale yellow. Scale bars equal 1 cm (see Color Plates, Fig. 6.3).

is typical for archosaurs, the large occipital venous sinus (an expansion of the dorsal longitudinal sinus that drains much of the brain and exits through the foramen magnum) overlies and hence obscures the details of the cerebellar, optic tectal, and brain stem regions (Sedlmayr 2002). Likewise the large ventral longitudinal sinus obscures the brainstem ventrally. Nevertheless, telencephalic portions of the brain, such as the olfactory bulbs and cerebral hemispheres, sufficiently fill their regions of the endocranial cavity that the endocast is a more faithful representation of their general size and shape. Although a vascular injection of the specimen at hand was not done, air fortuitously had entered the encephalic venous system post-mortem, providing the opportunity to digitally segment and visualize components of the dural sinus system that discriminate brain regions (Fig. 6.4). Remarkably, the pattern serendipitously recovered closely reflects the published accounts of Hochstetter (1906); van Gelderen (1924) and Hopson (1979). For example, the transverse sinus passes between the regions of the optic

tectum and otic capsule, and the sphenoparietal sinus passes between the cerebral hemisphere and tectum.

Figure 6.3 also illustrates the major neurovascular features of the endocast, such as the canals for the cranial nerves and cerebral carotid artery. It should be noted that virtually all of these canals also transmit veins from adjacent regions into the dural venous sinuses (Sedlmayr 2002). Structures of particular note include the facial nerve (CN VII), which splits into its hyomandibular ramus (chorda tympani) and its long palatine ramus. The trigeminal (Gasserian) ganglion is located outside the cranial cavity (i.e., extracranial), and its main branches – the ophthalmic (CN V₁), maxillary (CN V₂), and mandibular (CN V₃) nerves – are well-visualized, as are two lesser known branches: (1) the supraorbital ramus of the maxillary nerve (Holliday and Witmer 2007) and (2) the tympanic branch, which passes through the prootic bone to reach the tympanic cavity. This latter branch relates to another seldom-seen structure that is visible on the endocast, and that is the canal for

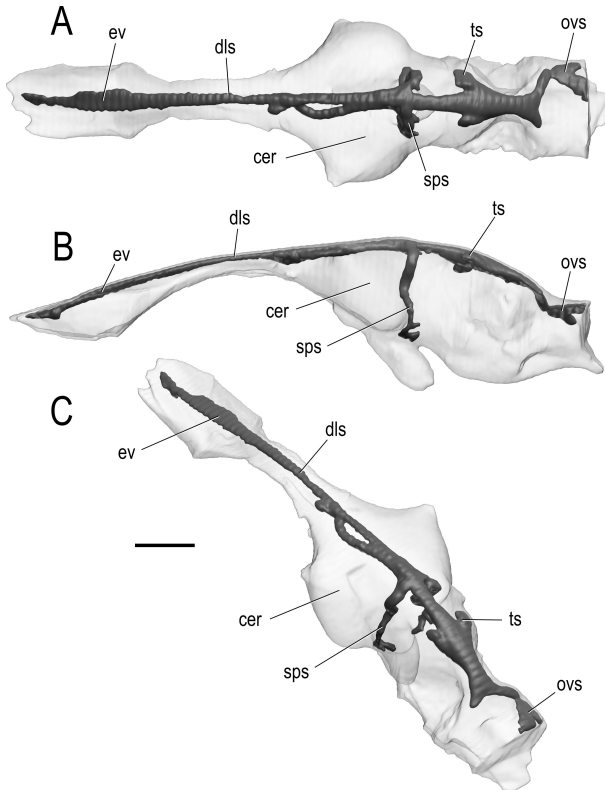


FIG. 6.4. Dural venous sinuses within the semitransparent cranial endocast of an Australian freshwater crocodile, *Crocodylus johnstoni* (OUVC 10425), derived from surface renderings of CT scan data. **A**, dorsal view. **B**, left lateral view. **C**, left caudodorsolateral view. Scale bar equals 1 cm.

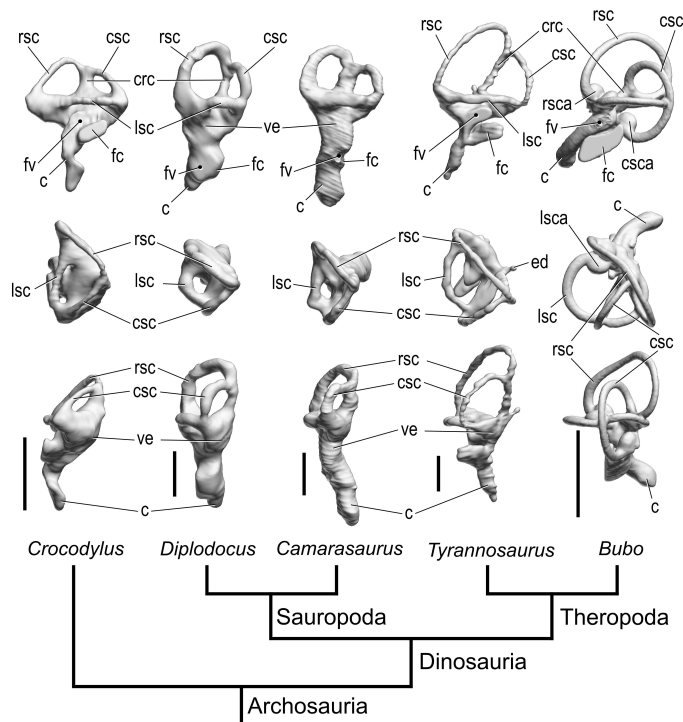


FIG. 6.5. Endosseous labyrinths of the left inner ears of the principal taxa discussed in the text, displayed on a diagram of their phylogenetic relationships. From left, the extant crocodylian *Crocodylus johnstoni* (OUVC 10425), the diplodocoid sauropod *Diplodocus longus* (CM 11161), the macronarian sauropod *Camarasaurus lentus* (CM 11338), the basal coelurosaurian theropod *Tyrannosaurus rex* (AMNH 5117), and the avian theropod (bird) *Bubo virginianus* (OUVC 10220). These sauropods and theropods are saurischian dinosaurs. The images are surface renderings of CT scan data. Top row: left lateral view. Middle row: dorsal view. Bottom row: caudal view. Orientations determined based on orientation of the labyrinth within the skull and with the lateral semicircular canal placed horizontally. Scale bars equal 1 cm.

the tympanic branches of the glossopharyngeal (CN IX) and vagus (CN X) nerves. Killian (1890) regarded these branches as joining with the tympanic branch of the trigeminal nerve mentioned above.

Just as the cranial endocast is a representation of dural form and not strictly the brain itself, the labyrinth does not record the membranous (endolymphatic) labyrinth and moreover does not truly record the ‘osseous’ labyrinth which traditionally includes the bony canals and walls; rather, it records the space just internal to the bone, and hence we apply the descriptor ‘endosseous.’ The endosseous labyrinth of the inner ear (Fig. 6.5) is fairly typical for extant crocodylians (we have comparable data for *Alligator*, other *Crocodylus*, *Gavialis*, and numerous fossil species), with a relatively simple, triangular vestibular apparatus dorsally and an elongate cochlea (lagena) ventrally. The strongly twisted cochlea no doubt corresponds

to the twisting of the basilar membrane described by Wever (1978). The cerebral carotid artery passes just lateral to the inflection point of the twist. The long slender columellae (stapes) also were visualized (Fig. 6.3) and mark the position of the fenestra vestibuli (ovalis) on the labyrinth. The bony braincase is pneumatized by air-filled diverticula of the pharynx, including a median pharyngeal diverticulum and paired pharyngotympanic (Eustachian) tubes (Fig. 6.6A,B). The general pattern determined from CT is generally similar to that presented by Owen (1850) and Colbert (1946b), although the one presented here is more complete in including the long siphonial tube that passes through the quadrate bone on its way to the articular bone of the lower jaw. Based on broader studies underway by D. L. Dufeau, the cranial pneumatic system of *C. johnstoni* is relatively reduced in comparison to other extant crocodylians.

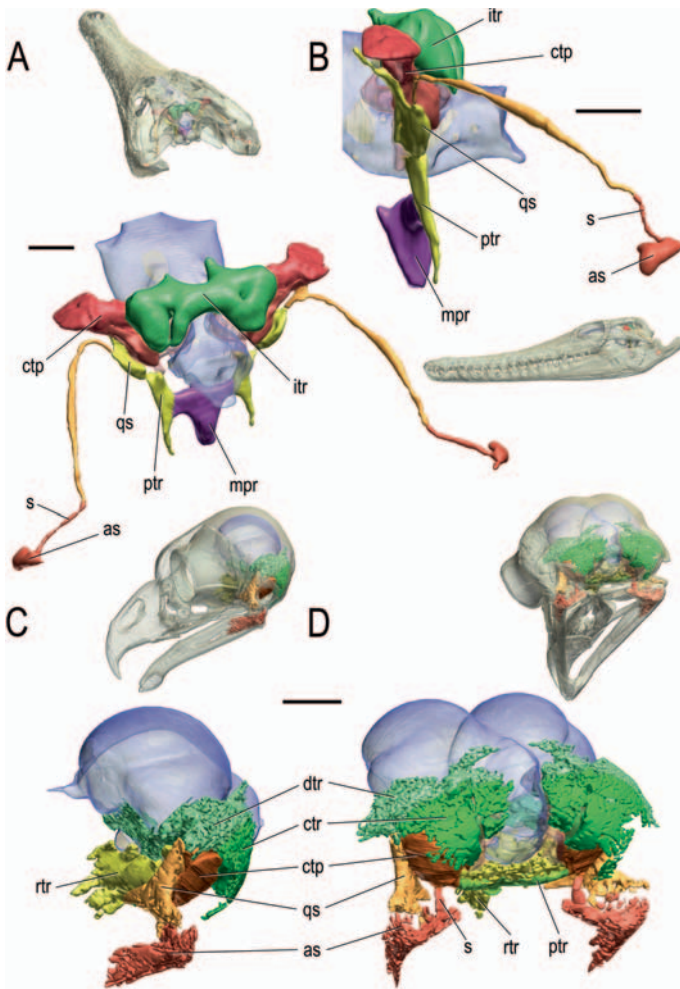


FIG. 6.6. Pneumatic sinuses of the braincase region of, (A–B), an Australian freshwater crocodile, *Crocodylus johnstoni* (OUVC 10425), and (C–D), a great horned owl, *Bubo virginianus* (OUVC 10220), viewed surrounding a semitransparent cranial endocast, derived from surface renderings of CT scan data. Thumbnail views of the whole skull are provided above the main image (except B, where it is below) to show the orientation of the main image. (A) *C. johnstoni* in left caudodorsolateral view. (B) *C. johnstoni* in left lateral view. (C) *B. virginianus* in left lateral view. (D) *B. virginianus* in left caudoventrrolateral view. Scale bars equal 1 cm (see Color Plates, Fig. 6.6).

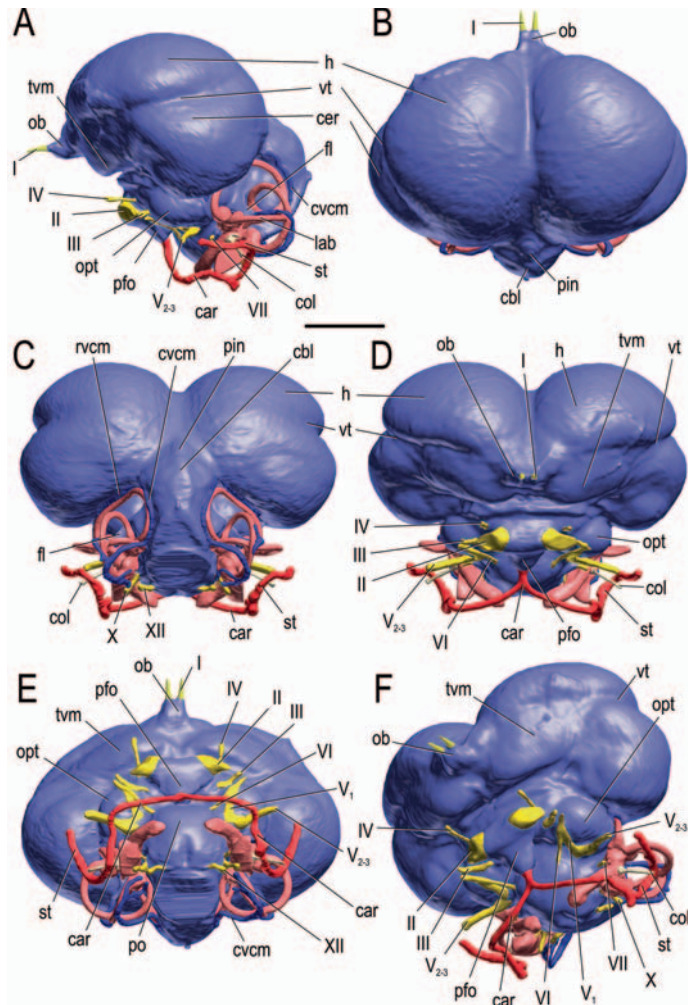
6.6 Extant Outgroups: *Bubo virginianus*, Great Horned Owl

Whereas the cranial endocast of the freshwater crocodile above bears only a superficial resemblance to the underlying brain, the endocast of *Bubo virginianus* (OUVC 10220; Fig. 6.7) closely resembles the form of the brain itself, as determined both by our dissection of a different specimen of *B. virginianus* (OUVC 10427) and Turner's (1891) illustration of a *B. virginianus* brain (see also Stingelin 1957, for photographs of the brains of four other owl species). This close resemblance results from the fact that avian meninges are very thin, and thus the large brain essentially fills the endocranial cavity (Jerison 1973; Iwaniuk and Nelson 2002). A major difference between the brain and endocast is that the expansive occipital

dural sinus obscures the cerebellar folia in the endocast. Major features of the endocast include (1) large cerebral hemispheres with a very large hyperpallium (Wulst), (2) small olfactory bulbs, (3) ventrolaterally displaced optic (mesencephalic) tecta (optic lobes), (4) small flocculi (cerebellar auricles), and (5) separate ophthalmic and maxillomandibular branches of the trigeminal nerve reflecting the intracranial position of the trigeminal ganglion. Avian brain terminology used here follows Breazile and Kuenzel (1993); Dubbeldam (1998), and Reiner et al. (2004).

The endosseous labyrinth of the inner ear is a very elongate and elaborate series of canals and swellings (Fig. 6.5), and, as with the brain, much more closely approximates the form of the underlying membranous labyrinth than does the endosseous labyrinth of crocodylians. The remarkable hearing capabilities of owls are well known, and

FIG. 6.7. Cranial endocast, endosseous labyrinth, and some endocranial vascular structures of a great horned owl, *Bubo virginianus* (OUVC 10220), derived from surface renderings of CT scan data. **A**, left lateral view. **B**, dorsal view. **C**, caudal view. **D**, rostral view. **E**, ventral view. **F**, left rostroventrolateral view. Color scheme: cranial endocast, blue; endosseous labyrinth, pink; nerve canals (most of which also transmit veins), yellow; smaller venous canals, dark blue; arterial canals, red; columella, pale yellow. Scale bar equals 1 cm (see Color Plates, Fig. 6.7).



their auditory physiology (particularly that of the barn owl, *Tyto alba*) has been very well studied (see reviews by Dooling et al. 2000; Gleich and Manley 2000; Gleich et al. 2004). The structure of the labyrinth itself, however, has been poorly documented in owls, apparently being limited to little more than a schematic drawing (Norberg 1978) and photographs of dissected osseous labyrinths (Tanturri 1933; Turkewitsch 1934).

The semicircular canals are very long and slender. As is almost always the case in birds (based on our CT-based studies of numerous other species), the rostral semicircular canal is the longest and prescribes an oval, whereas the caudal and lateral canals are shorter and more circular. The lateral canal communicates with not just the caudal canal but also the rostral canal. As Gray (1908) noted, perilymphatic communication of the lateral and caudal canals is the typical avian condition,

but he found the double-communication condition we report in *B. virginianus* to be quite rare (owls were not included in Gray's sample). The additional communication (between lateral and rostral canals) results in part from the relatively short crus communis, but also from the great length and excursion of the lateral and rostral canals that bring them close enough to communicate.

The footplate of the columella fits into the fenestra vestibuli of the skull, which opens to the base (dorsal end) of the cochlea. The cochlea itself is remarkably long and is curved such that it arcs around and ventral to the pontine portion of the endocast (Fig. 6.7C–F). The great length of the cochlea presumably relates to the presence of an elongate basilar membrane. The length of the basilar membrane is not recoverable from our data and has not been reported otherwise for great horned owls, but barn owls have the longest

basilar membranes recorded for birds (Gleich and Manley 2000).

The advantage of CT-based studies of the labyrinth is that structures can be easily viewed in relation to other anatomical systems (Fig. 6.7). For example, the elongate rostral semicircular canal is closely appressed to the cerebellum, overlies the optic tectum rostrally, and is partially overlain by the occipital pole of the cerebrum. In fact, the angulation of the rostral canal visible in dorsal view (Fig. 6.5, middle row) corresponds to the point where the canal passes from cerebellum to cerebrum (Fig. 6.7C), and probably has no relevance for vestibular function. The cerebellar flocculus enters the cage formed by the three canals, passing just rostral to the crus communis, but does not fill the cage, as it does in pterosaurs (Witmer et al. 2003). Much of the labyrinth is surrounded by and suspended within the paratympanic pneumatic sinuses, which is fairly typical for birds.

The pneumatic system itself is very extensive, much more so than in the freshwater crocodile described above, and only its more proximal portions are indicated in Fig. 6.6C–D. Unlike the crocodile, the pneumaticity of the braincase derives ultimately from the pharyngotympanic tubes. The five major tympanic diverticula observed in other birds (Witmer 1990, 1997) are present in great horned owls (see Norberg 1978, for another owl species). The quadrate and articular bones are extensively pneumatized. Another difference with crocodylians is that the siphonial tube in birds does not pass through the quadrate on its way to the articular. The caudal tympanic recess is broadly confluent with the very extensive dorsal tympanic recess. The rostral tympanic recess is also expansive and has a broad contralateral communication ventral to the brain cavity. This communication (known as the interaural pathway) has been implicated in the localization of sounds in space in birds generally, although its role in owls has been controversial (see Klump 2000, for a review).

6.7 Sauropod Dinosaurs: *Camarasaurus* and *Diplodocus*

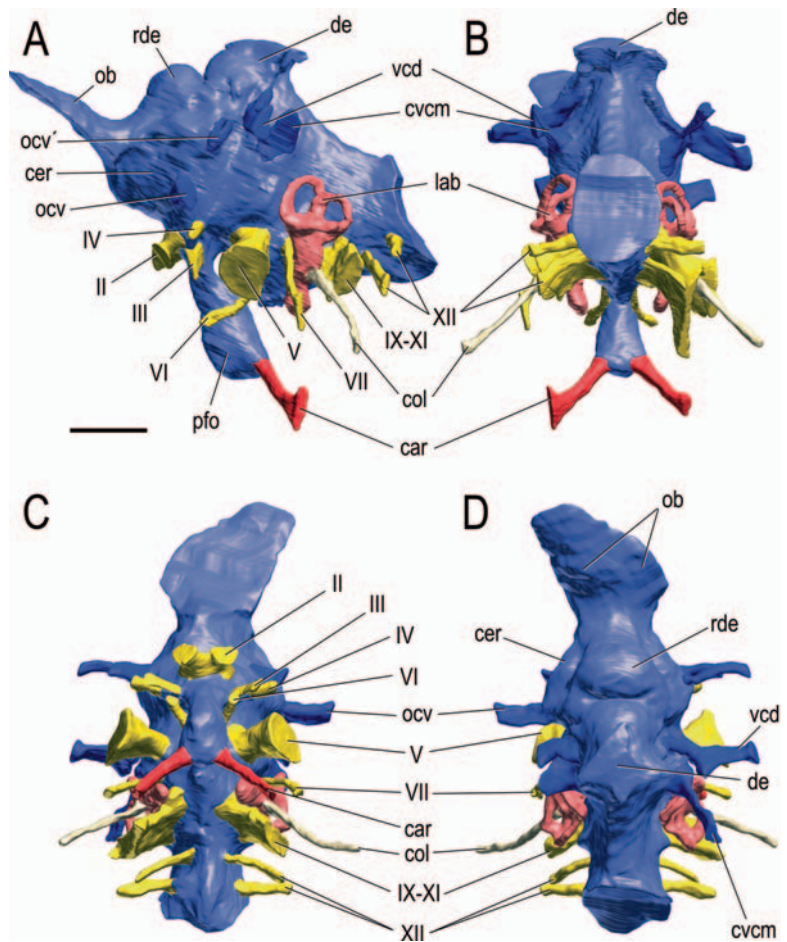
The first presentation of a digital cranial endocast for a sauropod can be credited to Franzosa (2004) in his unpublished doctoral dissertation; his work on a specimen of *Diplodocus* (HMS 175, formerly CM 662) largely agrees with ours. A few other papers, based on traditional physical endocasts,

also provide significant descriptions (Osborn 1912; Osborn and Mook 1921; Janensch 1935, 1936; Ostrom and McIntosh 1966; Hopson 1979; Chatterjee and Zheng 2002, 2005; Knoll et al. 2006). The endocasts presented here (Figs 6.8, 6.9) are the most complete published to date. Sauropods lacked the extensive paratympanic sinuses that pneumatized the braincases of the crocodile and owl above, and so the discussion will be limited to the endocast and labyrinth.

Sauropod endocasts in general and those of *Camarasaurus* (Fig. 6.8) and *Diplodocus* (Fig. 6.9) in particular are quite distinct from those of extant birds and crocodylians, but they are much more similar to those of crocodylians in that the brain does not fill the endocranial cavity. In fact, the endocasts of both sauropod taxa presented here suggest that the dura was very loose-fitting indeed, in that brain regions are difficult to discern. Part of this difficulty results from the fact that the endocranial region of most sauropods appears to have been highly vascular, with very large venous sinuses that created prominent grooves, recesses, and apertures within the bony endocranial surface. Again, as in crocodylians, the cerebral hemispheres and olfactory bulbs are the clearest, although even here only portions of the brain regions (e.g., the ventral and lateral surfaces of the cerebrum) are discernible. It should be pointed out that not all sauropods have such a loose dural envelope in that the endocasts of some titanosaurs from India (under study in collaboration with S. Chatterjee) have very clearly defined cerebral regions and a generally less complicated endocast.

From what can be discerned about brain structure, the new digital endocasts confirm much of what previously was known, in that sauropod brains were apparently relatively primitive in overall structure and certainly very small in relation to body size (metric data will be presented elsewhere). Our new studies, however, present the first view of the olfactory bulbs of sauropods. Although only the dorsal contour of the olfactory bulb can be observed due to lack of ossification of the flooring cartilages, criteria developed from the study of modern relatives and other dinosaurs specify the demarcation between olfactory bulb and nasal cavity. The bulb region is better preserved in *Diplodocus* (Fig. 6.9D) than in *Camarasaurus* (Fig. 6.8D), but in both cases the olfactory bulbs are relatively large in comparison to the rest of the endocast. As a result of the caudal retraction of the nasal cavity and concomitant telescoping

FIG. 6.8. Cranial endocast, endosseous labyrinth, and some endocranial vascular structures of the sauropod dinosaur, *Camarasaurus lentus* (CM 11338), derived from surface renderings of CT scan data. **A**, left lateral view. **B**, caudal view. **C**, ventral view. **D**, dorsal view. Color scheme: cranial endocast, blue; endosseous labyrinth, pink; nerve canals (most of which also transmit veins), yellow; smaller venous canals, dark blue; arterial canals, red; columella, pale yellow. Scale bar equals 2 cm (see Color Plates, Fig. 6.8).



ing of the braincase, the olfactory tracts are quite short, and the bulbs are strongly inclined relative to the main axis of the brain. Another prominent feature of the endocast is the large and pendant pituitary (hypophyseal) fossa. The large bony fossa housed much more than the pituitary itself, in that the cerebral carotids enter it ventrolaterally, the abducens and oculomotor nerves pass through it, and it receives large veins from the orbit (see below). Nevertheless, as Edinger (1942) noted, it is very reasonable to assume that at least part of the reason that these large-bodied dinosaurs had such large pituitary fossae was to house an enlarged pituitary.

The cranial nerve exits on the sauropod endocasts are generally very straightforward, and share a number of common features, many of which are primitive for archosaurs, if not sauropsids as a whole. Shared features, all of which are bilateral, include the following: (1) two canals for the hypoglossal nerve (CN XII); (2) a large ‘jugular’ aperture (sometimes called the ‘metotic foramen,’ see

discussion in Sampson and Witmer, 2007) through which passed the glossopharyngeal, vagus, and accessory nerves (CN IX–XI) and the jugular vein, and which housed part of the perilymphatic apparatus; (3) a single facial nerve (CN VII) canal; (4) a single canal for the trigeminal nerve which expands laterally as the swelling for the (extra-cranial) trigeminal ganglion; (5) the abducens nerve (CN VI) canal passes through the lateral portion of the pituitary fossa; (6) the oculomotor (CN III) and trochlear (IV) apertures are large, separate (or sharing an hour-glass-shaped fissure), and located in the infundibular region (where the pituitary fossa joins the main endocranial cavity); and (7) the optic nerve (CN II) has a broad separate aperture. The trigeminal arrangement merits comment in that none of the trigeminal branches are separate in these (or any other known) sauropods, which is unlike the situation in the extant archosaurs discussed above in which the ophthalmic nerve had its own canal. This is discussed further below.

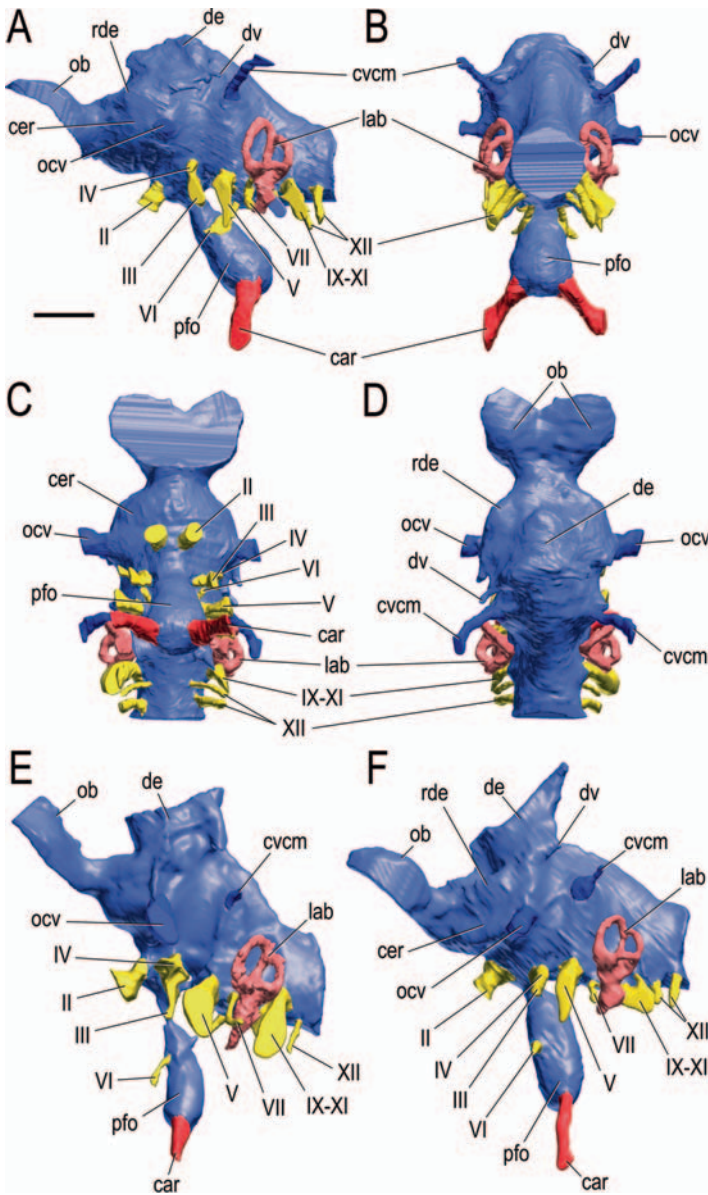


FIG. 6.9. Cranial endocast, endosseous labyrinth, and some endocranial vascular structures of the sauropod dinosaur, *Diplodocus longus*, derived from surface renderings of CT scan data. **A–D**, CM 3452. **E**, AMNH 694. **F**, CM 11161. **A**, **E**, **F**, left lateral view. **B**, caudal view. **C**, ventral view. **D**, dorsal view. Color scheme: cranial endocast, *blue*; endosseous labyrinth, *pink*; nerve canals (most of which also transmit veins), *yellow*; smaller venous canals, *dark blue*; arterial canals, *red*. Scale bar equals 2 cm (see Color Plates, Fig. 6.9).

There has been some confusion in the literature regarding the location of the trochlear nerve aperture. For example, Osborn (1912) identified in *Diplodocus* (AMNH 694) a large aperture between the orbitosphenoid and laterosphenoid as being for the trochlear nerve; the endocast he presented for this specimen has a corresponding swelling. This identification was subsequently followed by Hopson (1979), Galton (1985), and Franzosa (2004). Our findings, on the other hand, suggest that the aperture in question is a large venous channel and that the trochlear foramen is located more ventrally, directly above the oculomotor

foramen (Figs 6.8A,C, 6.9A,C). Our digital endocasts of both *Diplodocus* and *Camarasaurus* have three apertures along the laterosphenoid-orbitosphenoid contact: the oculomotor and trochlear foramina together ventrally and the venous channel displaced dorsally. This identification is supported by the fact that the trochlear foramen in some other saurischian dinosaurs (see Sampson and Witmer 2007) is in the same general region as the foramina for the optic, oculomotor, and abducens nerves, which makes sense given their related functions. It should be noted that Janensch (1935, 1936) showed a similar arrangement of

foramina for *Barosaurus*, but regarded the trochlear and oculomotor nerves as sharing a large foramen in *Dicraeosaurus*. Likewise, we have found both conditions in our broader sample, with, for example, the Indian titanosaur specimens ISIR 603 and ISIR 199 displaying separate but adjacent trochlear and oculomotor foramina and *Suuwassea emilieae* (ANSP 21122) displaying a common aperture for the two nerves, as in *Dicraeosaurus*.

The identity of the large, more dorsal foramen that formerly had been regarded as being for the trochlear nerve is not clear. Janensch (1935, 1936) regarded it as being homologous to the fenestra epioptica, an opening within the chondrocrania of most extant sauropsids. He further suggested that the aperture transmitted an encephalic vein, the ‘anterior cerebral vein.’ His assessment was followed by most workers, even those that thought the aperture also transmitted the trochlear nerve (e.g., White 1958; Galton 2001; Franzosa 2004). It is certain that a large vein drained from the orbit into the encephalic sinuses via this foramen, but homology with the embryonic fenestra epioptica of Gaupp (1900) is far from certain, as is the identity of the vein as the ‘anterior cerebral vein.’ This particular vein traverses the fenestra epioptica for only a brief period in some squamate embryos (van Gelderen 1924), and usually nothing traverses the fenestra epioptica (Shiino 1914). Thus, we instead apply the new term ‘orbitocerebral foramen,’ which transmitted a vein of the same name (Figs 6.8,6.9). Our CT-based studies have revealed that many groups of dinosaurs have fairly extensive anastomoses between veins within the cranial cavity (i.e., the dural sinuses) and the roof of the orbit (described for the theropod *Majungasaurus* in Sampson and Witmer 2007), and we regard the orbitocerebral foramen of sauropods as transmitting a particularly large such anastomosis.

The large size of the orbitocerebral foramen is just one of several pieces of evidence indicating that the endocranial cavity of many sauropods had an unusually complicated venous system. Virtually all of the cranial nerve foramina, particularly those opening into the orbit, are enlarged – certainly much larger than can be explained by transmitting just the nerve trunks. Given that the cranial nerve foramina in both clades of extant archosaurs (birds and crocodylians) transmit veins into the dural sinus system, it is reasonable to argue that not only did sauropods have such venous anastomoses but

also that they were very extensive. Other veins draining into the dural sinuses also appear to have been large. For example, *Camarasaurus* (CM 11338) has an additional orbitocerebral vein aperture on each side (Fig. 6.8A), and both the middle cerebral and dorsal head vein canals are well developed. These venous canals are more modest in specimens of *Diplodocus*, and the dorsal head vein and extra orbitocerebral vein canals are absent (Fig. 6.9).

Perhaps the most curious attribute of the cranial endocasts of most sauropods pertains to the dorsal dural expansion just caudal to the cerebral region. In the *Camarasaurus* and *Diplodocus* specimens at hand, there is a large median expansion with paired ventrolateral communications with venous features. In *Diplodocus*, these venous tracts communicate with the orbitocerebral apertures, whereas in *Camarasaurus* these tracts lead to the dorsal-head/middle-cerebral vein system. *Diplodocus* also has paired dural projections arising from the median dural expansion that extend blindly into the adjacent bone, and presumably represent diploic veins (Fig. 6.9A,B); these are much less developed in *Camarasaurus*. *Camarasaurus*, however, has an additional, median expansion rostral to and smaller than the one just discussed (Fig. 6.8A,D), and Chatterjee and Zheng (2005) illustrated a similar feature in a different specimen. *Diplodocus* also has a rostral dural feature, but here it takes the form of paired swellings that arc toward the olfactory tract cavity above the cerebral region (Fig. 6.9A,D).

The significance and soft-tissue relations of the dorsal dural expansion have been unclear. In many sauropods, this dural expansion is associated with an aperture (known as the parietal fontanelle) between the frontal and parietal bones, suggesting the presence of a pineal organ to some workers (Osborn 1912; Janensch 1935). Although some specimens of *Camarasaurus* have the aperture, CM 11338 lacks it, as reported by Gilmore (1925) and Madsen et al. (1995); we agree, although CT scanning reveals the bone to be very thin in this area. With regard to *Diplodocus*, both CM 11161 and AMNH 694 have large apertures, although the edges are broken, and it is hard to be certain of their veracity; CM 3452 clearly lacks an aperture. Whether or not there is an aperture ultimately is irrelevant to the inference of a pineal organ because extant dinosaurs (birds) and mammals have pineal glands yet lack skull roof

apertures, and such seems to be the case for at least some theropods, as well (Sampson and Witmer 2007). Hopson (1979), followed by a number of authors (e.g., Galton 1985, 2001; Wharton 2002), suggested the possibility that the large dorsal expansion was not dural but actually a gap or fontanelle that in life was plugged with persistent cartilage. We regard this hypothesis as falsified by the fact that the frontal and parietal are dermal elements, and thus there was no cartilage to 'persist.' The pineal hypothesis remains valid but obviously the volume of the dorsal expansions exceed that required for a pineal, and, combined with the other evidence for extensive dural sinuses, we regard the venous hypothesis as being the most likely (and does not preclude presence of the pineal).

The endosseous labyrinth of the inner ear has been reconstructed from the CT data for all four sauropod specimens presented here (and also for many other specimens in our broader sample). The labyrinths of *Camarasaurus* (Figs 6.5,6.8) and *Diplodocus* (Figs 6.5,6.9) are similar to each other, and closely resemble the only other sauropod labyrinth in the literature, that of *Brachiosaurus* (Janensch 1935; Clarke 2005). In general, the labyrinth is much more similar to that of the crocodile presented above than the bird, in that, as with the endocast, it provides only a rough approximation of the membranous labyrinth. For example, the ampullae are not at all apparent. Features of interest shared by *Camarasaurus* and *Diplodocus* include (1) a relatively very short lateral canal; (2) an enlarged vestibule; and (3) a relatively short cochlea. The cochlea superficially appears to be long, but the position of the fenestra vestibuli and columellar footplate fixes the vestibulocochlear junction, indicating that the vestibule was expanded ventrally well below the semicircular canal system (Fig. 6.5). Differences between the sauropod taxa in labyrinth structure are few, but the rostral semicircular canal is shorter and rounder in *Camarasaurus*, as opposed to that of *Diplodocus* and *Brachiosaurus*, which is taller and hence more oval. The endosseous labyrinths of the Indian titanosaurs in our sample resemble *Camarasaurus* in this regard. Based on outgroup comparison with the basal sauropodomorphs (e.g., *Massospondylus*, *Plateosaurus*) and theropods in our sample, the *Camarasaurus* rostral canal condition is derived, as are the short lateral canal and enlarged vestibule of sauropods generally.

6.8 Theropod Dinosaurs: *Tyrannosaurus*

The cranial endocast and endosseous labyrinth of the Cretaceous theropod *Tyrannosaurus rex* is presented briefly here (Fig. 6.10) to provide a counterpoint to those of the sauropods. A more detailed study of tyrannosaurs, including multiple specimens of *T. rex*, other tyrannosaurids, and a sampling of other theropods, is presented elsewhere. In general, the endocast still more closely resembles that of extant crocodylians in reflecting the contours of the brain only in the telencephalon. This condition is obviously primitive, but significant nonetheless in that tyrannosaurids are relatively closely related to birds. The cerebral region is enlarged relative to that in more basal theropods (Larsson et al. 2000; Hurlburt et al. in press), and expanded well beyond that observed in sauropods. Although the size of the olfactory lobes was greatly exaggerated in previous reports (e.g., Brochu 2000), the new corrected lobes presented here still are very enlarged in comparison to outgroups, and suggest that olfaction was behaviorally important to tyrannosaurs. With regard to the nerve trunks, the ophthalmic nerve is clearly separated from the maxillomandibular branch of the trigeminal nerve, suggesting that the point of their union – the trigeminal ganglion – is *internal* to the endocranial wall; thus, tyrannosaurids have the derived avian condition of an intracranial trigeminal ganglion rather than the primitive extracranial position exhibited by sauropods and crocodylians. Tyrannosaurs also resemble birds such as the owl in having a well developed middle-cerebral-vein/transverse-sinus system, yet retain the dorsal-head/middle-cerebral vein anastomoses described above for *Camarasaurus* and present in other theropods (Sampson and Witmer 2007).

In comparison to the other endosseous labyrinths discussed here, the tyrannosaur labyrinth (Fig. 6.5) is intermediate between that of the owl and crocodile in that the semicircular canals are long and slender, the ampullar regions are apparent (although not nearly as distinct as in the owl), and the cochlea is elongate. The air sinuses that pneumatize the braincase region of tyrannosaurs are extensive (Fig. 6.11), and share many attributes with those of advanced theropods and birds (Witmer 1997). As in birds, such as the owl, there

FIG. 6.10. Cranial endocast, endosseous labyrinth, and some endocranial vascular structures of the theropod dinosaur, *Tyrannosaurus rex* (AMNH 5117), derived from surface renderings of CT scan data. **A**, left lateral view. **B**, dorsal view. **C**, ventral view. Color scheme: cranial endocast, *blue*; endosseous labyrinth, *pink*; nerve canals (most of which also transmit veins), *yellow*; smaller venous canals, *dark blue*; arterial canals, *red*. Scale bar equals 2 cm (see Color Plates, Fig. 6.10).

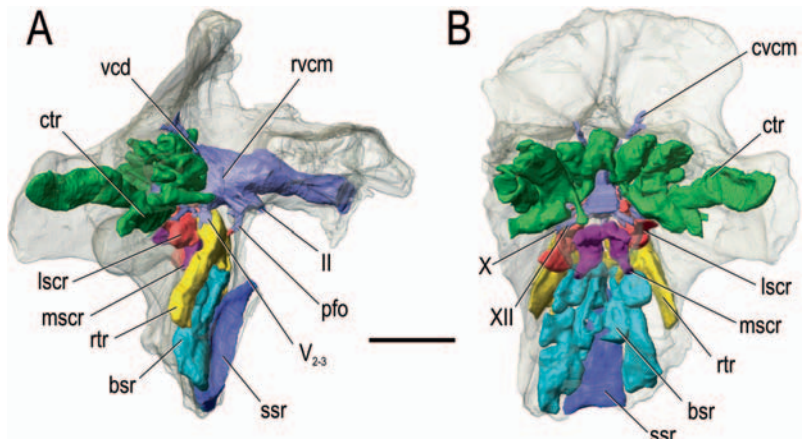
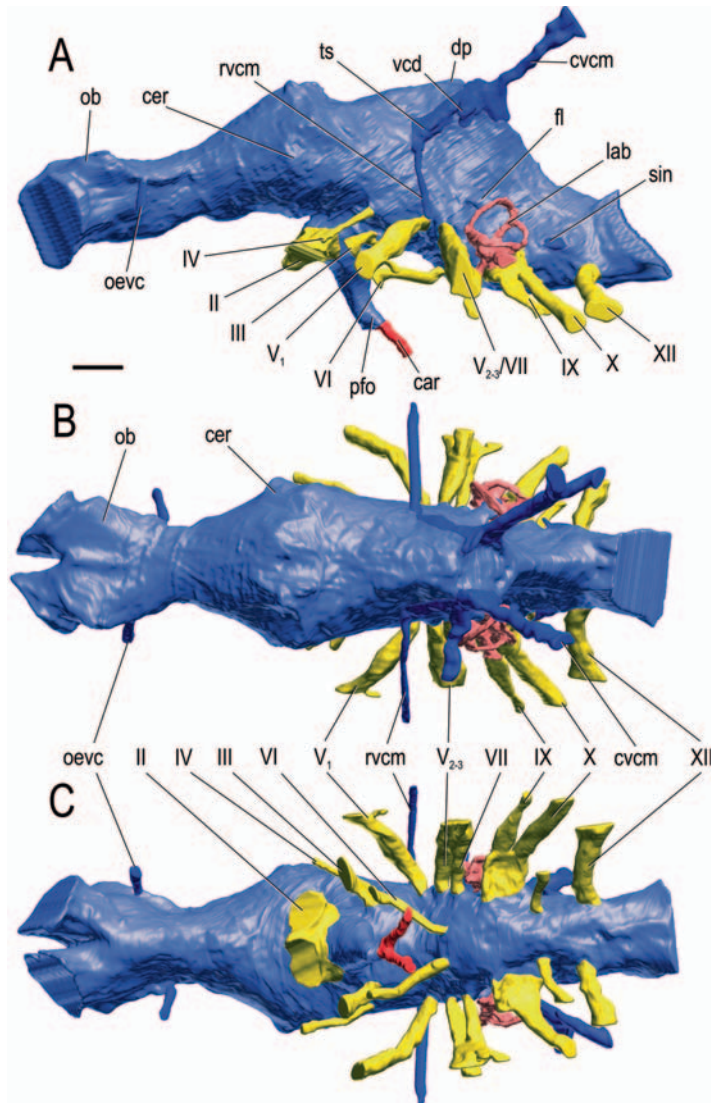


FIG. 6.11. Pneumatic sinuses and cranial endocast within the semi-transparent bony braincase of the theropod dinosaur, *Tyrannosaurus rex* (AMNH 5117), derived from surface renderings of CT scan data. **A**, right lateral view. **B**, caudal view. Scale bar equals 10 cm (see Color Plates, Fig. 6.11).

is a broad communication of the contralateral rostral tympanic recesses below the brain cavity in tyrannosaurs. As in crocodylians, there is broad contralateral communication above the brain cavity, as well, but these are via non-homologous sinuses.

6.9 Discussion

CT scanning indeed provides a means of ‘looking inside’ an object, which is a useful thing to do whether the object is a modern owl or an ancient dinosaur skull. But the combination of CT with digital segmentation and 3D visualization has provided a new anatomical tool that rivals the invention of the scalpel with regard to scientific impact. In the present case, we have employed these techniques to digitally dissect the anatomical structures of an extant crocodile and bird, as well as sauropod and tyrannosaur dinosaurs. Our figures convey the illustrative power of these approaches, but here we seek to discuss the bearing these findings have for the sensorineural interpretation of these two very different kinds of dinosaurs. Although *Tyrannosaurus* lived some 80 million years after *Camarasaurus* and *Diplodocus* and thus these are not strictly ‘predator and prey,’ tyrannosaurids and comparable sauropods were sympatric at least in the southwestern United States and in Mongolia (Weishampel et al. 2004), and so the comparison has some validity beyond heuristic value.

6.9.1 Brain Size and Structure

That dinosaurs have small brains relative to body size is hardly a new discovery, and, as mentioned earlier, full quantitative analysis will be presented elsewhere. Nevertheless, we will present some representative values here for comparison. For example, the endocast of *Diplodocus* (CM 11161) has a mass of about 110 g; assuming a body mass of about 13,000 kg (Henderson 1999), endocast size is about 0.001% of body size. For *Tyrannosaurus* (AMNH 5117), the endocast size is about 424 g, which, assuming a body mass of about 5000 kg (Erickson et al. 2004), accounts for about 0.008% of body size. More meaningful comparisons look at allometric scaling of these parameters, and Jerison (1973) proposed the metric of Encephalization Quotient (EQ) which provides a comparison of actual brain size relative to the

expected brain size of an animal of that body size. We use Hurlburt’s (1996; see also Hurlburt et al. in press) modified equations for reptiles (REQ). Both Jerison and Hurlburt accounted for the fact that the cranial endocast is an overestimate of the true brain size by halving endocast volume to estimate brain volume (i.e., brain size is 50% of endocast size), admittedly a very rough measure, but illuminating nonetheless. The REQ for *Tyrannosaurus* is 2.7, which means that its brain was almost three times the size expected for a reptile of its size. The REQ for *Diplodocus* is 0.41, which means that its brain was less than half the expected size. Thus, and this is no real surprise either, the brain power of the predator exceeds that of the prey. Typically this can be understood to reflect mostly the neural requirements for predation (principally sensory integration), but *Tyrannosaurus* presumably had some cognitive capabilities that sauropods lacked. In fact, the cerebral region of *Tyrannosaurus* is not only more visible in the endocasts than in the sauropods, but it is also measurably expanded over theropod dinosaurs other than the advanced birdlike maniraptorans (Larsson et al. 2000); Hurlburt et al. in press).

In terms of structure, again much of the brain form is hidden beneath the loose dural envelope. Nevertheless, *Tyrannosaurus* and the sauropods both had relatively large olfactory bulbs. As mentioned above, even with the newly corrected size of the olfactory bulbs, *Tyrannosaurus* still has large olfactory bulbs, and this enlargement is a derived feature requiring explanation. Jerison (1973) presented the ‘principle of proper mass,’ which states that the amount of neural tissue (for us, gross size of a brain region) is proportional to the amount or importance of the functions carried out by those tissues (see Butler and Hodos [2005] for an up-to-date corroboration of this principle). Thus, it is reasonable to assume that the apomorphically large size of the olfactory bulbs in tyrannosaurs suggest that the sense of smell was behaviorally important. The new finding presented here is that at least some sauropods also exhibit large olfactory bulbs, again suggesting the importance of olfactory cues. It remains obscure exactly which behaviors of these dinosaurs required a heightened sense of smell, and there is no reason to believe that a single explanation applies to both groups. The explanation sometimes advanced for *Tyrannosaurus* – namely, habitual if not obligate scavenging (e.g., Horner 1994) – obviously did not

apply to sauropods, and in fact, there is ample reason to regard active predation, not pure scavenging, as accounting for the sensorineural adaptations of tyrannosaurs.

6.9.2 Inner Ear: Hearing, Balance, Eye Movements, and Head Posture

There are striking differences between sauropods and tyrannosaurs in the form of the endosseous labyrinth of the inner ear, and these differences relate to a number of different biological traits. The cochlea is the part of the inner ear associated with hearing, and tyrannosaurs have a long cochlea whereas sauropods have a short one. Given that the extant birds and crocodylians in our sample have elongate cochleae (see above), it is tempting to regard the short sauropod cochlea as the derived condition; we are testing that hypothesis in our broader study. The length of the bony cochlea is directly related to the length of the sensory epithelium (the basilar membrane). As a result, cochlear length has been used as a rough proxy for the hearing capabilities of birds and crocodylians (Wever 1978; Gleich and Manley 2000). Thus, it would seem that discrimination of auditory stimuli were more important to tyrannosaurs than to sauropods. Moreover, given the relationships set forth by Gleich et al. (2005), it is reasonable to suggest that tyrannosaurs emphasized, in particular, the reception of low-frequency air-borne sounds. This interpretation is consistent with the extensive middle ear pneumaticity that we report above for tyrannosaurs, because these air sinuses reduce the mechanical stiffness of the middle ear air space at low frequencies (by allowing greater vibrational movement of the columellar apparatus), as well as affecting resonant properties and hence frequency-dependent amplification of sounds (Pickles 1988). Extant birds and crocodylians (such as the owl and crocodile above) also have extensive paratympanic pneumaticity, and experimental studies show that these animals also generally emphasize low frequencies (Dooling et al. 2000). Significantly, sauropods essentially lack middle ear pneumaticity, which, in combination with their short cochleae, supports the notion that fine discrimination of air-borne sounds (particularly low frequencies) was not as important for sauropods.

The upper part of the inner ear – the vestibule and semicircular canals – comprises the vestibular

apparatus and is associated with the sense of balance or equilibrium. Again, we see marked morphological differences in these attributes between sauropods and tyrannosaurs: sauropods have short, thick semicircular canals and a large vestibule, whereas tyrannosaurs have elongate, slender canals and a more modest vestibule. Comparison with extant archosaurs shows that the semicircular canals of sauropods are more similar to crocodylians (but perhaps even more reduced) whereas those of *Tyrannosaurus* are more like birds (but not approaching the condition of most birds, and certainly not owls). Semicircular canals sense angular acceleration or turning movements of the head, and increased sizes (length, radius of curvature, arc, etc.) have been linked to such behavioral patterns as enhanced agility and aerobic/acrobatic ability in birds and primates (Tanturri 1933; Turkewitsch 1934; Spoor and Zonneveld 1998; Spoor 2003; Spoor et al. 2007). It is tempting – and perhaps not unjustified – to suggest that the canal differences between these two dinosaur groups relate to tyrannosaurs being active, agile bipeds and the sauropods being slow-moving quadrupeds. However, how such morphological differences of the vestibular system relate to locomotor modes is somewhat obscure for vertebrates generally (Hullar 2006).

Certainly, even if the links to locomotor behavior are less direct (Graf and Klam 2006), the relationship of labyrinth form to eye movements and gaze-stabilization mechanisms is well established in the context of the vestibulo-ocular and vestibulo-collic reflexes (VOR and VCR; see Spoor 2003; Witmer et al. 2003; Spoor et al. 2007; and references therein). The VOR and VCR involves coordination and compensatory movements of the eyes, head, and neck so that a target moving relative to the subject remains fixed and in-focus on the retina. These mechanisms, and hence the semicircular canal system, are best developed in animals for which tracking movements of the eyes are at a premium, which, in fact, tends to include predatory animals, agile animals, and animals that engage in aerobic, acrobatic, and rapid arboreal locomotion. In this context, the expanded canals of *Tyrannosaurus* can be interpreted as reflecting an enhanced VOR/VCR in comparison to sauropods and extant crocodylians, and further suggesting that rapid tracking movements of the eyes were important behaviorally.

The apomorphically short, stubby canals of sauropods, on the other hand, particularly the very short lateral canal, must be reflecting decreased importance of or reliance on compensatory movements of the eyes and head. Reduction of the semicircular canals in cetaceans has been linked to reduced eye mobility, eye musculature, and neck mobility (see Spoor and Zonneveld 1998; Spoor 2003; and references therein), but we have no objective evidence to suggest that these explanations pertain to sauropods. Sauropod orbits are large, their scleral ossicles (when preserved, as in CM 11338 and CM 11161) suggest an unreduced eyeball, and their necks are the longest known among vertebrates (although perhaps less flexible than once had been thought; Stevens and Parrish 2005a). Rather it would seem that sauropods simply did not engage in rapid eye, head, and neck movements. This behavioral change is consistent with reduction or even absence of a discernible flocculus in most sauropods, the presence of which has been linked to the VOR and VCR in other archosaurs (see Witmer et al. 2003 and references therein). The strong reduction of the lateral canal further suggests that mediolateral eye and head movements, in particular, were less important, which may be consistent with inferred feeding behaviors involving sagittal (dorsoventral) movements of the head (Barrett and Upchurch 1994).

There is a large body of literature (see Witmer et al. 2003) relating the orientation of the lateral semicircular canal to the 'alert' posture of the head, such that when animals are alert and their senses heightened, they tend to hold their heads in an orientation that places the lateral canal roughly horizontal. Hullar (2006) noted that whereas many of the claims relating labyrinth form to locomotory differences are problematic, the links to head posture are well founded. Our team has demonstrated that alert postures of dinosaurs and other archosaurs (as determined by orienting the lateral canal horizontally in a semi-transparent skull in lateral view) were rather variable, even within a clade (Witmer et al. 2003; Sampson and Witmer 2007). Turning to the extant taxa presented in this paper, the bird in our sample, *Bubo virginianus*, has an alert posture that is fairly strongly down-turned, such that the long axis of the skull is declined about 30° below the horizontal (Fig. 6.2). The alert head posture as determined from the lateral canal has not been published previously for any owl, but we can report that the

declination angle in a barn owl (*Tyto alba*) in our sample is only about 15°. By contrast, a bald eagle (*Haliaeetus leucocephalus*) in our sample has an almost completely horizontal alert posture (declination angle of about 0°). Likewise, the alert posture of the crocodile in our sample, *Crocodylus johnstoni*, is basically horizontal (Fig. 6.2), and this is true for the other extant crocodylians in our sample (e.g., *C. moreletii*, *Alligator mississippiensis*, *Gavialis gangeticus*). Thus, although birds exhibit a wide range of alert head postures, crocodylians are relatively homogenous.

Turning to the fossil taxa presented in this paper, *Tyrannosaurus rex* has a very slightly down-turned alert posture of the head (5–10°; Fig. 6.2), and that of *Majungasaurus* is also basically horizontal (Sampson and Witmer 2007). However, a number of other theropod dinosaurs have much more strongly down-turned postures, including another tyrannosaurid (*Nanotyrannus*: 25–30°). In the above cited papers, we related these differences in alert posture among theropods to the demands of maintaining a maximal binocular field of view by clearing the snout and/or bony orbital rugosities from the field of view. Similar arguments were also made for differences in head posture between two pterosaurs (Witmer et al. 2003). Of the two sauropods presented here, *Camarasaurus* has a much more horizontal skull, with a declination angle of less than 10°, whereas *Diplodocus* has a very strongly down-turned posture (about 45°, averaging values from CM 3452 and CM 11161; Fig. 6.2). In this case, explanations for these differences may have less to do with binocularity, in part because the very large snout would still obstruct frontal vision in *Camarasaurus*, and in part because, based on first principles, we would not predict a strong selective premium for binocularity in these non-predaceous animals. These differences between these two sauropods, however, do agree with other morphological findings from the skull base and neck, and the differing head postures have been related to differences in feeding strategies (Barrett and Upchurch 1994; Fiorillo 1998; Stevens and Parrish 2005b).

Acknowledgments

We thank Roland Frey and Hideki Endo for their invitation to participate in this volume. We thank Matthew Lamanna and Amy Henrici (CM,

Pittsburgh) for loan of *Camarasaurus* and *Diplodocus* skulls, and Mark Norell and Carl Mehling (AMNH, New York City) for loan of *Diplodocus* and *Tyrannosaurus* skulls. For providing the specimen of *Crocodylus johnstoni*, we thank John Hutchinson (Royal Veterinary College, London), Kent Vliet, David Kledzik, and the St. Augustine Zoological Park, Florida. We have benefited from discussions with many colleagues at many institutions, including in particular Christopher Brochu, Thomas Carr, Sankar Chatterjee, Philip Currie, Jon Franzosa, Peter Galton, Casey Holliday, James Hopson, Grant Hurlburt, Harry Jerison, Timothy Rowe, Jayc Sedlmayr, Paul Sereno, Kent Stevens, and Takanobu Tsuihiji. We also benefited from Tsuihiji's careful reading of a draft of this manuscript. For help with CT scanning, we thank Heather Rockhold, RT, and O'Bleness Memorial Hospital, in Athens, Ohio. For funding, we acknowledge National Science Foundation grants IBN-9601174, IBN-0343744, and IOB-0517257, and the Ohio University College of Osteopathic Medicine.

References

- Barrett PM, Upchurch P (1994) Feeding mechanisms in *Diplodocus*. *Gaia* 10:195–203
- Breazile JE, Kuenzel WJ (1993) Systema nervosum centrale. In: Baumel JJ (ed.) *Handbook of Avian Anatomy: Nomina Anatomica Avium*, 2nd edn. Publications of the Nuttall Ornithological Club No 23, Cambridge, pp 493–554
- Buchholtz EA, Seyfarth E-A (1999) The gospel of the fossil brain: Tilly Edinger and the science of paleoneurology. *Brain Res Bull* 48:351–361
- Brochu CA (2000) A digitally rendered endocast for *Tyrannosaurus rex*. *J Vertebr Paleontol* 20:1–6
- Brochu CA (2003) Osteology of *Tyrannosaurus rex*: insights from a nearly complete skeleton and high-resolution computed tomographic analysis of the skull. *J Vertebr Paleontol Memoir* 7:1–140
- Butler AB, Hodos W (2005) *Comparative vertebrate neuroanatomy: evolution and adaptation*, 2nd edn. Wiley-Interscience, Hoboken
- Carlson WD, Rowe T, Ketcham RA, Colbert MW (2003). Geological applications of high-resolution x-ray computed tomography in petrology, meteoritics and palaeontology. In: Mees F, Swennen R, Van Geet M, Jacobs P (eds) *Applications of x-ray computed tomography in the geosciences*. Geological Society, London, pp 7–22
- Chatterjee S, Zheng Z (2002) Cranial anatomy of *Shunosaurus*, a basal sauropod dinosaur from the Middle Jurassic of China. *Zool J Linn Soc* 136:145–169
- Chatterjee S, Zheng Z (2005) Neuroanatomy and dentition of *Camarasaurus lentus*. In: Tidwell V, Carpenter K (eds) *Thunder-Lizards: the Sauropodomorph Dinosaurs*. Indiana University Press, Bloomington, IN, pp 199–211
- Clarke AH (2005) On the vestibular labyrinth of *Brachiosaurus brancai*. *J Vestib Res* 15:65–71
- Colbert EH (1946a) *Sebecus*, representative of a peculiar suborder of fossil Crocodylia from Patagonia. *Bull Am Mus Nat Hist* 87:217–270
- Colbert EH (1946b) The Eustachian tubes in the Crocodylia. *Copeia* 1946:12–14
- Conroy GC, Vannier MW (1984) Noninvasive three-dimensional computer imaging of matrix-filled fossil skulls by high-resolution computed tomography. *Science* 226:456–458
- Domínguez Alonso P, Milner AC, Ketcham RA, Cookson MJ, Rowe TB (2004) The avian nature of the brain and inner ear of *Archaeopteryx*. *Nature* 430:666–669
- Dooling RJ, Lohr B, Dent ML (2000). Hearing in birds and reptiles. In: Dooling RJ, Fay RR, Popper AN (eds) *Comparative hearing: birds and reptiles*. Springer, New York, pp 308–359
- Dubbeldam JL (1998). Birds. In: Nieuwenhuys R, ten Donkelaar HJ, Nicholson C (eds) *The central nervous system of vertebrates*, Vol. 3. Springer-Verlag, New York City, pp 1525–1636
- Edinger T (1942) The pituitary body in giant animals fossil and living: a survey and a suggestion. *Q Rev Biol* 17:31–45
- Edinger T (1975) Paleoneurology 1804–1966. An annotated bibliography. *Adv Anat Embryol Cell Biol* 49:1–258
- Erickson GM, Makovicky PJ, Currie PJ, Norell MA, Yerby SA, Brochu CA (2004) Gigantism and comparative life-history parameters of tyrannosaurid dinosaurs. *Nature* 430:772–775
- Fiorillo AR (1998) Dental microwear patterns of the sauropod dinosaurs *Camarasaurus* and *Diplodocus*: evidence for resource partitioning in the Late Jurassic of North America. *Hist Biol* 13:1–16
- Franzosa JW (2004) Evolution of the brain in Theropoda (Dinosauria). Unpublished PhD dissertation. University of Texas, Austin, Texas, 357 pp.
- Franzosa J, Rowe T (2005) Cranial endocast of the Cretaceous theropod dinosaur *Acrocanthosaurus atokensis*. *J Vertebr Paleontol* 25:859–864
- Galton PM (1985) Cranial anatomy of the prosauropod dinosaur *Plateosaurus* from the Knollenmergel (Middle Keuper, Upper Triassic) of Germany. II. All the cranial material and details of soft-part anatomy. *Geologica et Palaeontologica* 19:119–159
- Galton PM (1989) Crania and endocranial casts from ornithomimid dinosaurs of the families Dryosauridae and Hypsilophodontidae (Reptilia: Ornithischia). *Geologica et Palaeontologica* 23:217–239
- Galton PM (2001). Endocranial casts of the plated dinosaur *Stegosaurus* (Upper Jurassic, western USA): a complete undistorted cast and the original specimens of Othniel Charles Marsh. In: K Carpenter (ed.) *The armored dinosaurs*. Indiana University Press, Bloomington, IN, pp 103–129
- Gaupp E (1900) Das Chondrocranium von *Lacerta agilis*: ein Beitrag zum Verständnis des Amniotenschädels. *Anatomische Hefte* 14:435–592

- van Gelderen C (1924) Die Morphologie der Sinus durae matris. Erster Teil. Die vergleichende Ontogenie der neurokraniellen Venen der Anamnier und Reptilien. Zeitschrift für Anatomie und Entwicklungsgeschichte 73:541–605
- Gilmore CW (1925) A nearly complete articulated skeleton of *Camarasaurus*, a saurischian dinosaur from the Dinosaur National Monument Utah. Mem Carnegie Mus 10:353–367
- Gleich O, Manley GA (2000). The hearing organ of birds and Crocodilia. In: Dooling RJ, Fay RR, Popper AN (eds) Comparative hearing: birds and reptiles. Springer, New York, pp 70–138
- Gleich O, Fischer FP, Köppl C, Manley GA (2004). Hearing organ evolution and specialization: archosaurs. In: Manley GA, Popper AN, Fay RR (eds) Evolution of the vertebrate auditory system. Springer, New York, pp 224–255
- Gleich O, Dooling RJ, Manley GA (2005) Audiogram, body mass, and basilar papilla length: correlations in birds and predictions for extinct archosaurs. Naturwissenschaften 92:595–598
- Graf W, Klam F (2006) Le système vestibulaire: anatomie fonctionnelle et comparée, évolution et développement. Comptes Rendus Palevol 5:637–655
- Gray AA (1908) The labyrinth of animals, including mammals, birds, reptiles and amphibians, Vol. 2. Churchill, London
- Henderson DH (1999) Estimating the masses and centers of mass of extinct animals by 3-D mathematical slicing. Paleobiology 25:88–106
- Hochstetter F (1906) Beiträge zur Anatomie und Entwicklungsgeschichte des Blutgefäßsystems der Krokodile. Reise in Ostafrika. Wissenschaftliche Ergebnisse 4:1–139
- Holliday CM, Witmer LM (2007) Archosaur adductor chamber evolution: integration of musculoskeletal and topological criteria in jaw muscle homology. J Morphol 268:457–484
- Holliday CM, Ridgely RC, Balanoff AM, Witmer LM (2006) Cephalic vascular anatomy in flamingos (*Phoenicopterus ruber*) based on novel vascular injection and computed tomographic imaging analyses. Anat Rec 288A:1031–1041
- Hopson JA (1979). Paleoneurology. In: Gans C (ed.) Biology of the reptilia, Vol 9, Neurology A. Academic Press, New York, pp 39–146
- Horner JR (1994) Steak knives, beady eyes, and tiny little arms (a portrait of *T. rex* as a scavenger). In: Rosenberg GD, Wolberg DL (eds) Dino fest. Paleontological Society Special Publication 7, Knoxville, TN, pp 157–164
- Hullar TE (2006) Semicircular canal geometry, afferent sensitivity, and animal behavior. Anat Rec 288A:4656–472
- Hurlburt GR (1996) Relative brain size in Recent and fossil amniotes: determination and interpretation. PhD Dissertation, University of Toronto, Toronto, Ontario, Canada, 250 pp.
- Hurlburt GR, Ridgely RC, Witmer LM (in press). Relative size of brain and cerebrum in *Tyrannosaurus rex*: an analysis using brain-endocast quantitative relationships in extant alligators. In: Parrish JM, Henderson M, Currie PJ, Koppelhus E (eds) Origin, systematics, and paleobiology of the tyrannosauridae. Northern Illinois University Press
- Iwaniuk AN, Nelson JE (2002) Can endocranial volume be used as an estimate of brain size in birds. Can J Zool 80:16–23
- Janensch W (1935) Die Schädel der Sauropoden *Brachiosaurus*, *Barosaurus* und *Dicraeosaurus* aus den Tendaguru-Schichten Deutsch-Ostafrikas. Palaeontographica, Supplementum VII 1:147–297
- Janensch W (1936) Über Bahnen von Hirnvenen bei Saurischiern und Ornithischiern, sowie einigen anderen fossilen und rezenten Reptilien. Palaeontologische Zeitschrift 18:181–198
- Jerison HJ (1973) Evolution of the brain and intelligence. Academic Press, New York
- Killian G (1890) Die Ohrmuskeln des Krokodiles nebst vorläufigen Bemerkungen über die Homologie des Musculus stapedius und des Stapes. Jenaische Zeitschrift für Naturwissenschaft 24:632–656
- Klump GM (2000) Sound localization in birds. In: Dooling RJ, Fay RR, Popper AN (eds) Comparative hearing: birds and reptiles. Springer, New York, pp 249–307
- Knoll F, Galton PM, López-Antoñanzas R (2006) Paleoneurological evidence against a proboscis in the sauropod dinosaur *Diplodocus*. Geobios 39:215–221
- Kundrát M (2007) Avian-like attributes of a virtual brain model of the oviraptorid *Conchoraptor gracilis*. Naturwissenschaften 94:499–504
- Kurochkin EN, Saveliev SV, Postnov AA, Pervushov EM, Popov EV (2006) On the brain of a primitive bird from the Upper Cretaceous of European Russia. Paleontol J 40:655–667
- Larsson HCE (2001) Endocranial anatomy of *Carcharodontosaurus saharicus* (Theropoda: Allosauroidea) and its implications for theropod brain evolution. In: Tanke DH, Carpenter K (eds) Mesozoic vertebrate life. Indiana University Press, Bloomington, IN, pp 19–33
- Larsson HCE, Sereno PC, Wilson JA (2000) Forebrain enlargement among nonavian theropod dinosaurs. J Vertebr Paleontol 30:615–618
- Macrini TE, Rowe T, Archer M (2006) Description of a cranial endocast from a fossil platypus, *Obdurodon dicksoni* (Monotremata, Ornithorhynchidae), and the relevance of endocranial characters to monotreme monophyly. J Morphol 267:1000–1015
- Madsen JH, McIntosh JS Jr, Berman DS (1995) Skull and atlas-axis complex of the Upper Jurassic sauropod *Camarasaurus* Cope (Reptilia: Saurischia). Bull Carnegie Mus Nat Hist 31:1–116
- Maisey JG (2005) Braincase of the Upper Devonian shark *Cladoides wildungensis* (Chondrichthyes, Elasmobranchii), with observations on the braincase in early chondrichthyans. Bull Am Mus Nat Hist 288: 1–103
- Marino L, Uhen MD, Pyenson ND, Frohlich B (2003) Reconstructing cetacean brain evolution using computed tomography. Anat Rec (Part B) 272B:107–117
- Newton ET (1888) On the skull, brain, and auditory organ of a new species of pterosaurian (*Scaphognathus purdoni*), from the Upper Lias near Whitby Yorkshire. Philos Trans R Soc Lond B 179:503–537

- Norberg RA (1978) Skull asymmetry, ear Structure and function, and auditory localization in Tengmalm's Owl, *Aegolius funereus* (Linne). *Philos Trans R Soc Lond B Biol Sci* 282:325–410
- Osborn HF (1912) Crania of *Tyrannosaurus* and *Allosaurus*. *Mem Am Mus Nat Hist* 1:1–30
- Osborn HF, Mook CC (1921) *Camarasaurus*, *Amphicoelias*, and other sauropods of Cope. *Mem Am Mus Nat Hist* 3:247–387
- Ostrom JH, McIntosh JS (1966) Marsh's dinosaurs. The collections from Como Bluff. Yale University Press, New Haven, CT
- Owen R (1850) On the communication between the cavity of the tympanum and the palate in the Crocodilia (gavials, alligators and crocodiles). *Philos Trans R Soc Lond* 140:521–527
- Pickles JO (1988) An introduction to the physiology of hearing, 2nd edition. Academic Press, New York City, NY
- Radinsky LB (1968) A new approach to mammalian cranial analysis, illustrated by examples of prosimian primates. *J Morphol* 124:167–180
- Reiner A, Perkel DJ, Bruce L, Butler AB, Csilag A, Kuenzel W, Medina L, Paxinos G, Shimizu T, Striedter GF, Wild M, Ball GF, Durand S, Güntürkün O, Lee DW, Mello CV, Powers A, White SA, Hough G, Kubikova L, Smulders TV, Wada K, Dugas-Ford J, Husband S, Yamamoto K, Siang C, Yu J, Jarvis ED (2004) Revised nomenclature for avian telencephalon and some related brainstem nuclei. *J Comp Neurol* 473:377–414
- Rogers SW (1998) Exploring dinosaur neuropaleobiology: viewpoint computed tomography scanning and analysis of an *Allosaurus fragilis* endocast. *Neuron* 21:673–679
- Rogers SW (1999) *Allosaurus*, crocodiles, and birds: evolutionary clues from spiral computed tomography of an endocast. *Anat Rec* 257:162–173
- Rogers SW (2005) Reconstructing the behaviors of extinct species: an excursion into comparative paleoneurology. *Am J Med Genet* 134A:349–356
- Sampson SD, Witmer LM (2007) Craniofacial anatomy of *Majungasaurus crenatissimus* (Theropoda: Abelisauridae) from the Late Cretaceous of Madagascar. *Society of Vertebrate Paleontology Memoir* 8. *J Vertebr Paleontol* 27(Suppl. 2):32–102
- Sedlmayr JC (2002) Anatomy, evolution, and functional significance of cephalic vasculature in Archosauria. Ph. D. dissertation, Ohio University, 398 pp
- Shiino K (1914) Studien zur Kenntnis des Wirbeltierkopfes. I. Das Chondrocranium von *Crocodylus* mit Berücksichtigung der Gehirnnerven und der Kopfgefäße. *Anatomische Hefte* 50:257–381
- Spoor F (2003) The semicircular canal system and locomotor behaviour, with special reference to hominin evolution. In: Franzen JL, Köhler M, Moyà-Solà S (eds), *Walking upright*. Courier Forschungsinstitut Senckenberg 243, Stuttgart, pp 93–104
- Spoor F, Zonneveld F (1998) Comparative review of the human bony labyrinth. *Yearb Phys Anthropol* 41:211–251
- Spoor F, Garland T Jr, Krovitz G, Ryan TM, Silcox MT, Walker A (2007) The primate semicircular canal system and locomotion. *Proc Natl Acad Sci* 104:10808–10812
- Stensiö EA (1963) The brain and cranial nerves in fossil lower craniate vertebrates. *Skrifter utgitt av Det Norske Videnskaps-Akademi i Oslo. I. Matematisk-naturvidenskapelig klasse Ny; serie no 13*, pp 1–120
- Stevens KA, Parrish JM (2005a) Digital reconstructions of sauropod dinosaurs and implications for feeding. In: Curry Rogers K, Wilson JA (eds) *The sauropods: evolution and paleobiology*. University of California Press, Berkeley, CA, pp 178–200
- Stevens KA, Parrish JM (2005b) Neck posture, dentition, and feeding strategies in Jurassic sauropod dinosaurs. In: Tidwell V, Carpenter K (eds) *Thunder-lizards: the sauropodomorph dinosaurs*. Indiana University Press, Bloomington, IN, pp 213–232
- Stingelin W (1957) Vergleichend morphologische Untersuchungen am Vorderhirn der Vögel auf cytologischer und cytoarchitektonischer Grundlage. Verlag Helbing & Lichtenhahn, Basel
- Tanturri V (1933) Zur Anatomie und Physiologie des Labyrinthes der Vögel. *Monatsschrift für Ohrenheilkunde und Laryngo-Rhinologie* 67:1–27
- Turkewitsch BG (1934) Zur Anatomie des Gehörorgans der Vögel (Canales semicirculares). *Zeitschrift für Anatomie und Entwicklungsgeschichte* 103:551–608
- Turner CH (1891) Morphology of the avian brain. *J Comp Neurol* 1:39–92, 265–286
- Weishampel DB, Barrett PM, Coria RA, Loeuff J, Xu X, Zhao X, Sahni A, Goman EMP, Noto CR (2004) Dinosaur distribution. In: Weishampel DB, Dodson P, Osmólska H (eds), *The dinosauria*, 2nd edn. University of California Press, Berkeley, CA, pp 517–606
- Wever EG (1978) The reptile ear. Its structure and function. Princeton University Press, Princeton, NJ
- Wharton DS (2002) The evolution of the avian brain. Ph. D. dissertation, University of Bristol, UK
- White TR (1958) The braincase of *Camarasaurus lentus* (Marsh). *J Paleontol* 32:477–494
- Witmer LM (1990) The craniofacial air sac system of Mesozoic birds (Aves). *Zool J Linn Soc* 100:327–378
- Witmer LM (1995). The Extant Phylogenetic Bracket and the importance of reconstructing soft tissues in fossils. In: Thomason JJ (ed.) *Functional morphology in vertebrate paleontology*. Cambridge University Press, New York, pp 19–33
- Witmer LM (1997) Craniofacial air sinus systems. In: Currie PJ, Padian K (eds) *Encyclopedia of dinosaurs*. Academic Press, New York, pp 151–159
- Witmer LM, Ridgely RC (in press) The Cleveland tyrannosaur skull (*Nanotyrannus* or *Tyrannosaurus*): new findings based on CT scanning, with special reference to the braincase. *Kirtlandia*
- Witmer LM, Chatterjee S, Franzosa J, Rowe T (2003) Neuroanatomy of flying reptiles and implications for flight, posture and behavior. *Nature* 425:950–953

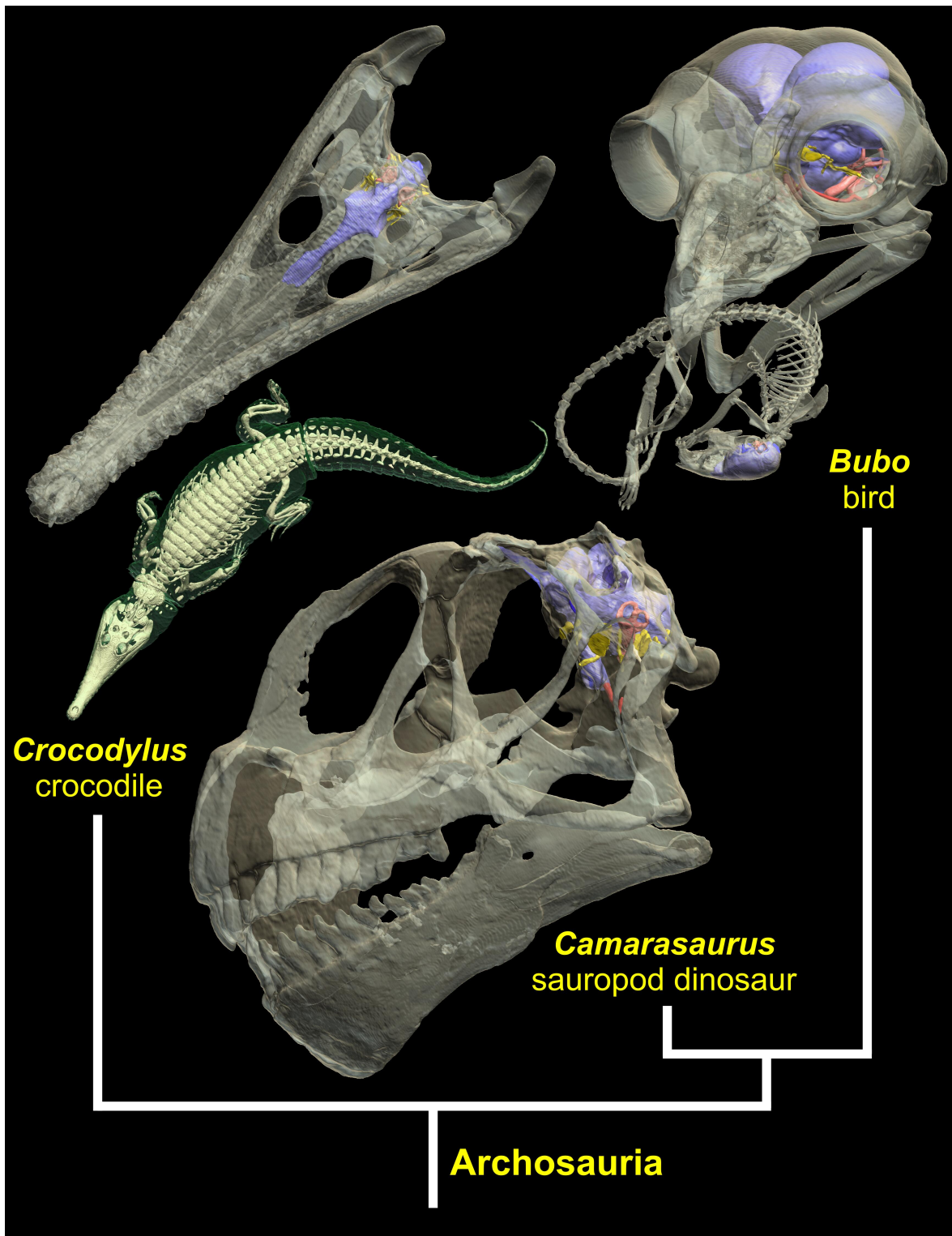


FIG. 6.1. The extant phylogenetic bracket (Witmer 1995) of nonavian dinosaurs, as exemplified by the sauropod dinosaur *Camarasaurus lentus* (CM 11338, in left lateral view). The extant outgroups of the fossil taxa provide information on attributes such as soft-tissue morphology and behavior that are not preserved in the fossils. The extant outgroups of nonavian dinosaurs are crocodylians (as exemplified by *Crocodylus johnstoni*, OUV 10425, in dorsal view) and birds (as exemplified by *Bubo virginianus*, OUV 10220, in left rostralateral view with *Mus musculus* [OUV 10449] in its jaws). The images are surfaces renderings of CT scan data, with the skull rendered semitransparent revealing the cranial endocast (in blue) and other structures.

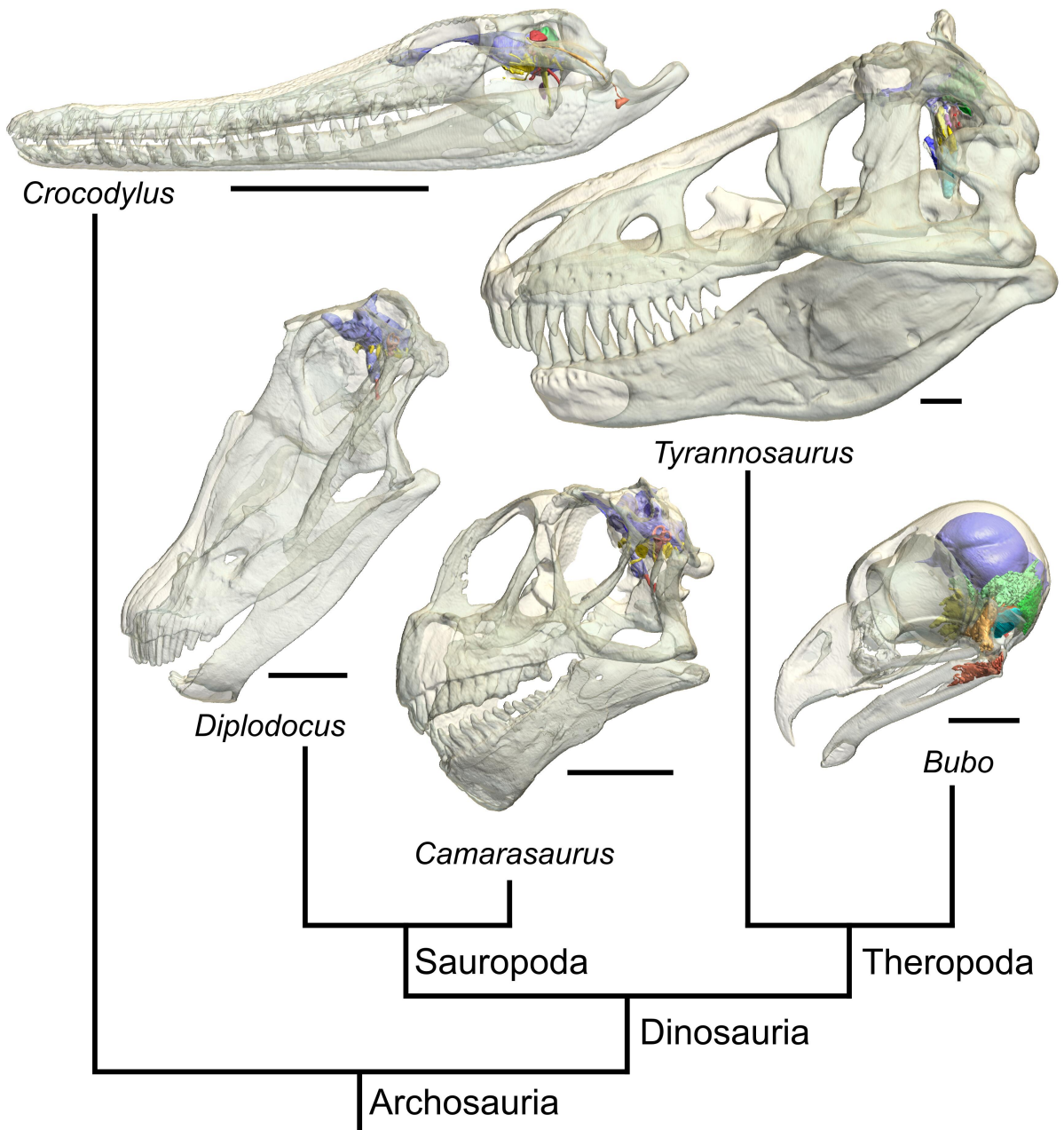


FIG. 6.2. Diagram of the phylogenetic relationships of the principal taxa discussed in the text. From left, the extant crocodylian *Crocodylus johnstoni* (OUVC 10425), the diplodocoid sauropod *Diplodocus longus* (CM 11161), the macronarian sauropod *Camarasaurus lentus* (CM 11338), the basal coelurosaurian theropod *Tyrannosaurus rex* (AMNH 5117), and the avian theropod (bird) *Bubo virginianus* (OUVC 10220). These sauropods and theropods are saurischian dinosaurs. The images are surface renderings of CT scan data. Bony skulls are depicted as transparent, revealing such internal structures as the brain cast, labyrinth, and pneumatic sinuses. All skulls are oriented in their 'alert' postures, determined by orienting the skull such that the lateral semicircular canal is horizontal. Scale bars equal 10 cm, except that for *B. virginianus* which equals 2 cm.

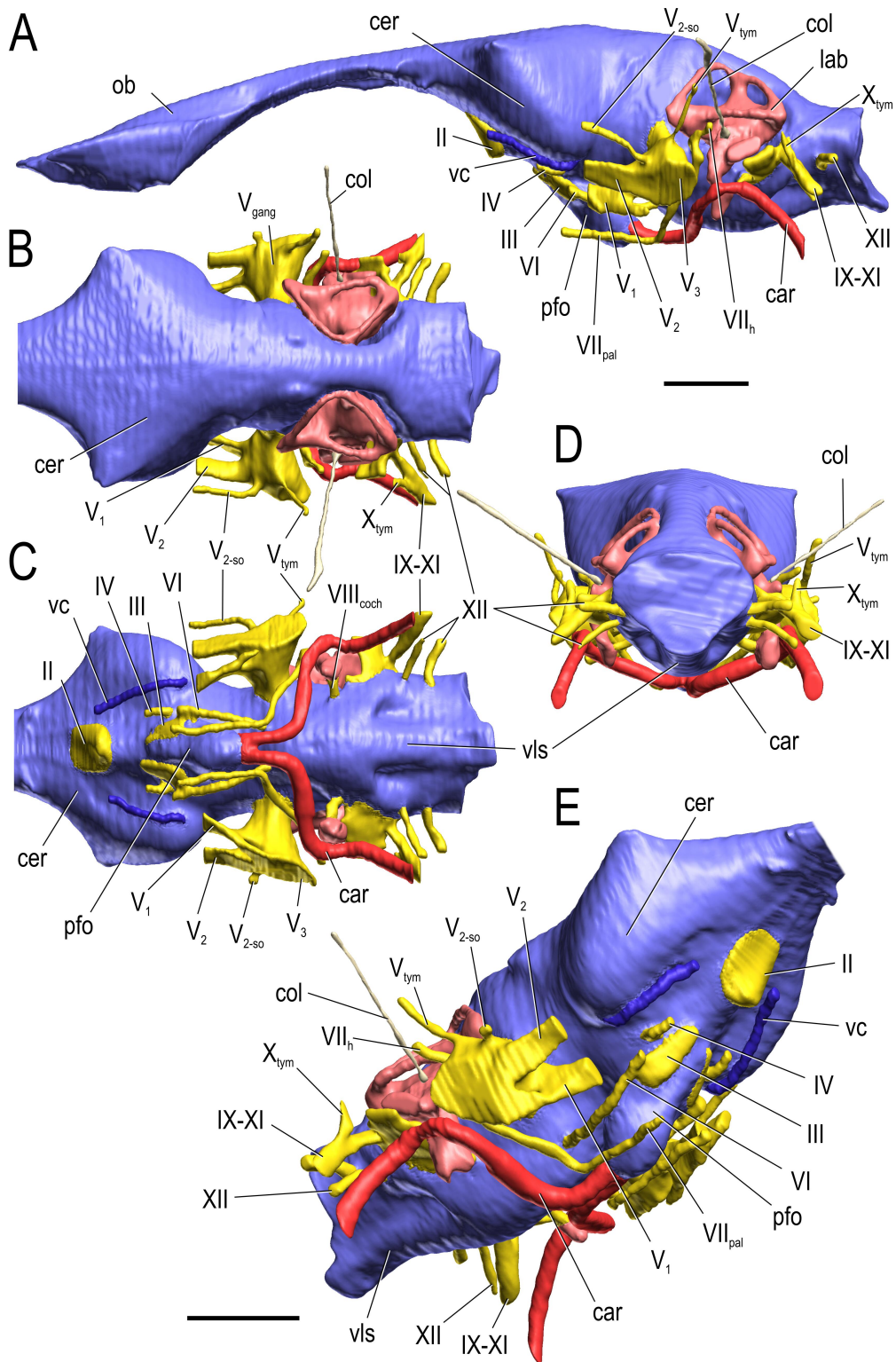


FIG. 6.3. Cranial endocast, endosseous labyrinth, and some endocranial vascular structures of an Australian freshwater crocodile, *Crocodylus johnstoni* (OUVC 10425), derived from surface renderings of CT scan data. **A**, left lateral view. **B**, dorsal view, with olfactory tract truncated. **C**, ventral view, with olfactory tract truncated. **D**, caudal view. **E**, right rostro-ventrolateral view. Color scheme: cranial endocast, blue; endosseous labyrinth, pink; nerve canals (most of which also transmit veins), yellow; smaller venous canals, dark blue; arterial canals, red; columella, pale yellow. Scale bars equal 1 cm.

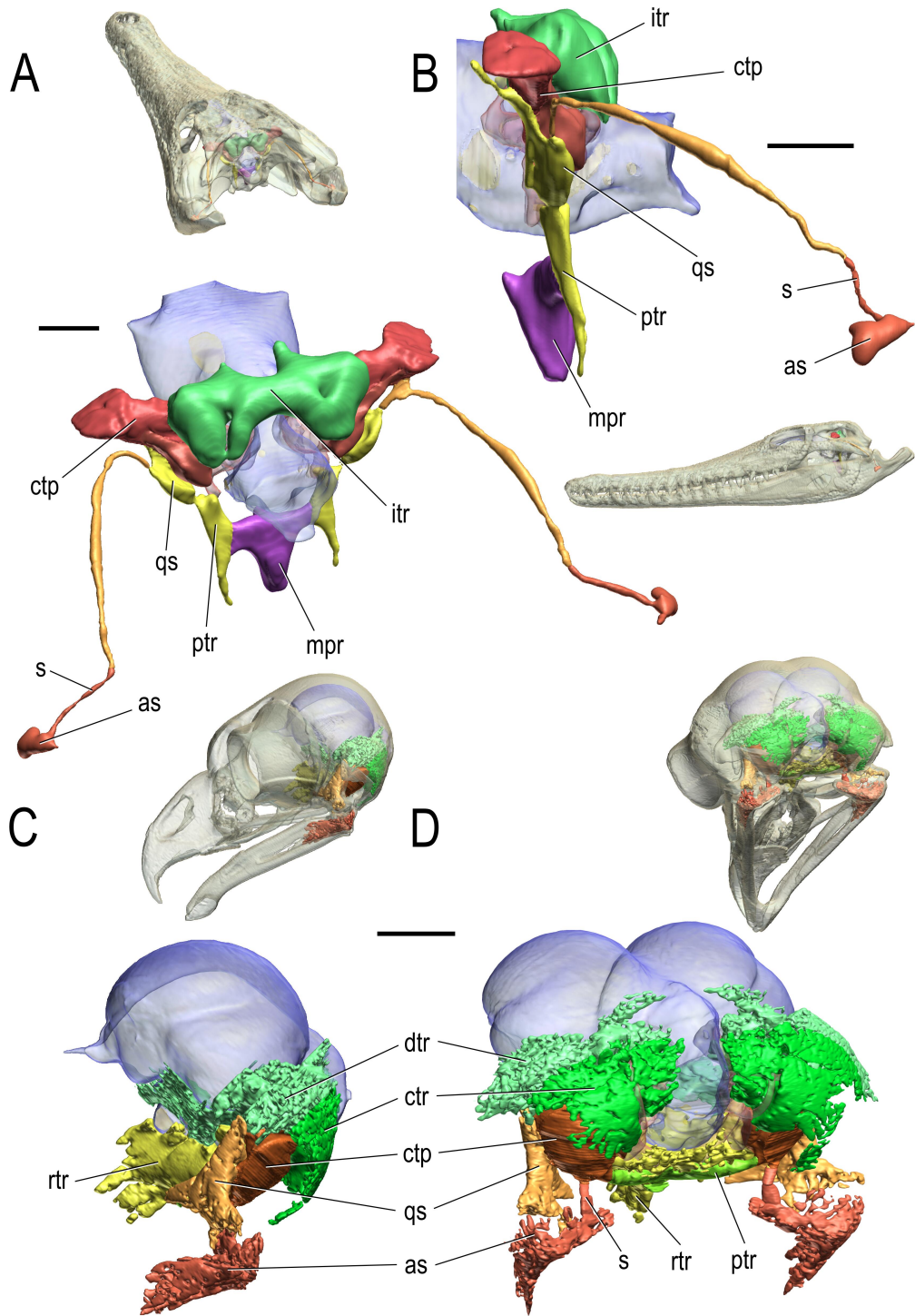


FIG. 6.6. Pneumatic sinuses of the braincase region of, (A–B), an Australian freshwater crocodile, *Crocodylus johnstoni* (OUVC 10425), and (C–D), a great horned owl, *Bubo virginianus* (OUVC 10220), viewed surrounding a semitransparent cranial endocast, derived from surface renderings of CT scan data. Thumbnail views of the whole skull are provided above the main image (except B, where it is below) to show the orientation of the main image. (A) *C. johnstoni* in left caudodorsolateral view. (B) *C. johnstoni* in left lateral view. (C) *B. virginianus* in left lateral view. (D) *B. virginianus* in left caudoventrolateral view. Scale bars equal 1 cm.

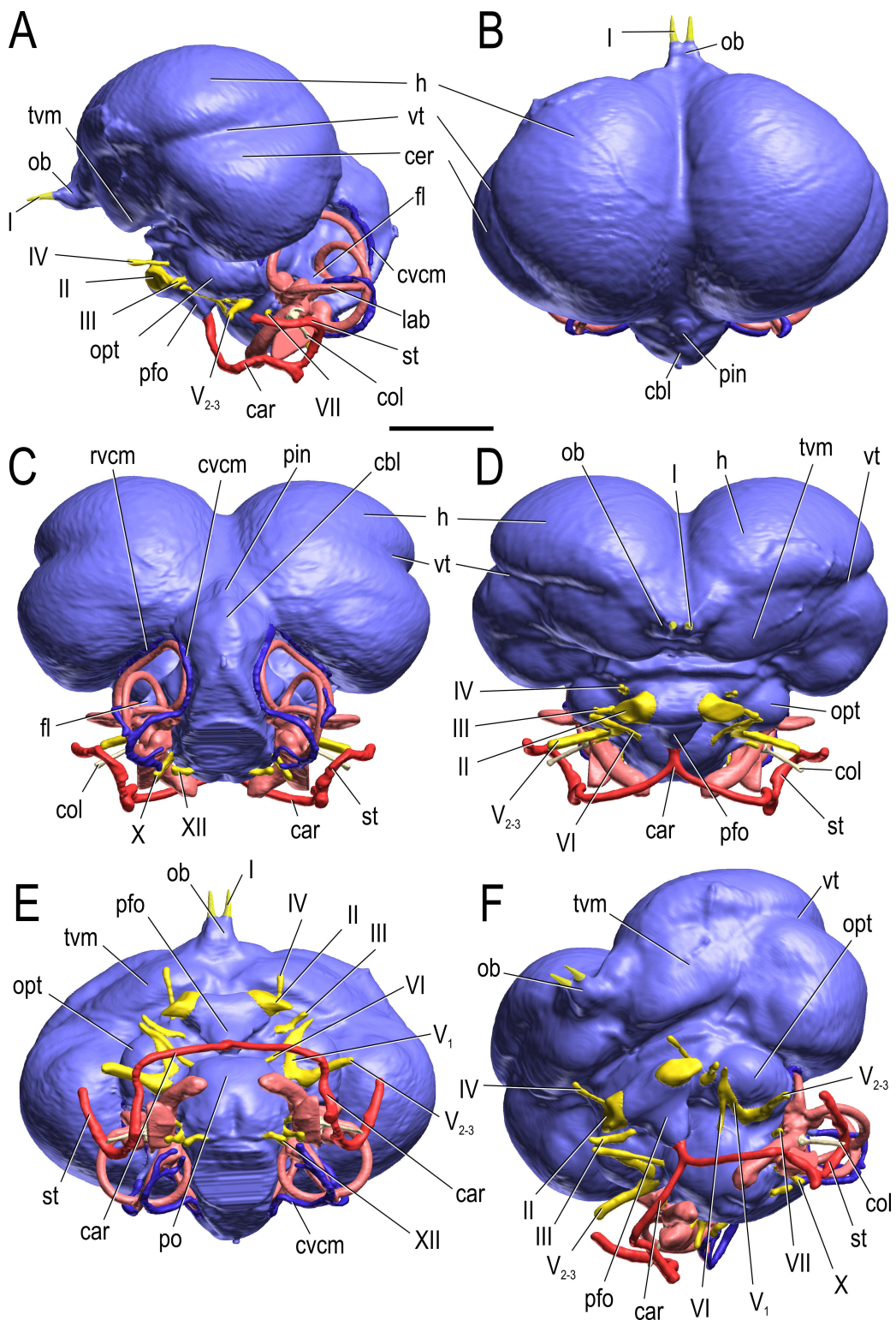


FIG. 6.7. Cranial endocast, endosseous labyrinth, and some endocranial vascular structures of a great horned owl, *Bubo virginianus* (OUVC 10220), derived from surface renderings of CT scan data. **A**, left lateral view. **B**, dorsal view. **C**, caudal view. **D**, rostral view. **E**, ventral view. **F**, left rostroventrolateral view. Color scheme: cranial endocast, blue; endosseous labyrinth, pink; nerve canals (most of which also transmit veins), yellow; smaller venous canals, dark blue; arterial canals, red; columella, pale yellow. Scale bar equals 1 cm.

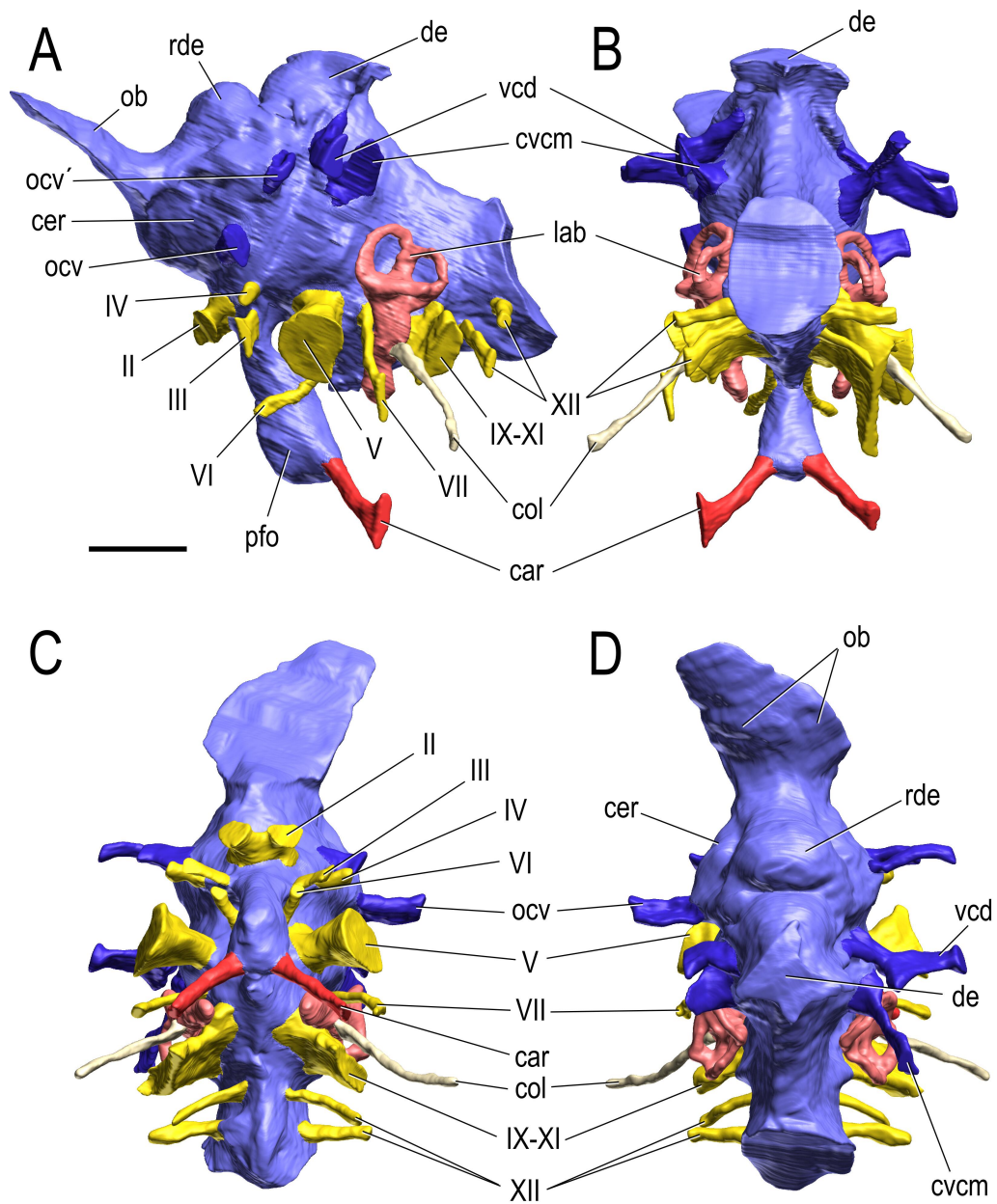


FIG. 6.8. Cranial endocast, endosseous labyrinth, and some endocranial vascular structures of the sauropod dinosaur, *Camarasaurus lentus* (CM 11338), derived from surface renderings of CT scan data. **A**, left lateral view. **B**, caudal view. **C**, ventral view. **D**, dorsal view. Color scheme: cranial endocast, blue; endosseous labyrinth, pink; nerve canals (most of which also transmit veins), yellow; smaller venous canals, dark blue; arterial canals, red; columella, pale yellow. Scale bar equals 2 cm.

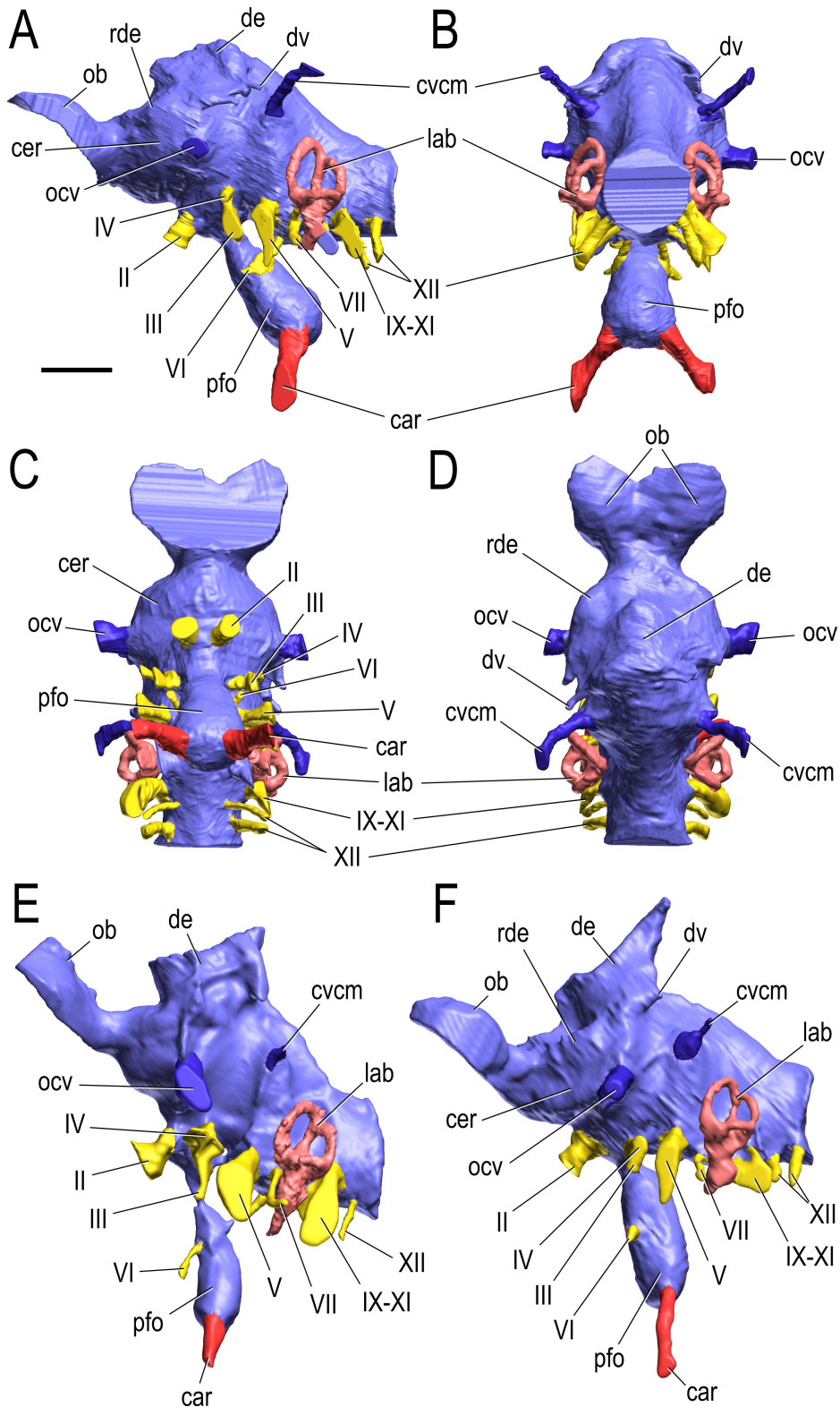


FIG. 6.9. Cranial endocast, endosseous labyrinth, and some endocranial vascular structures of the sauropod dinosaur, *Diplodocus longus*, derived from surface renderings of CT scan data. **A–D**, CM 3452. **E**, AMNH 694. **F**, CM 11161. **A**, **E**, **F**, left lateral view. **B**, caudal view. **C**, ventral view. **D**, dorsal view. Color scheme: cranial endocast, *blue*; endosseous labyrinth, *pink*; nerve canals (most of which also transmit veins), *yellow*; smaller venous canals, *dark blue*; arterial canals, *red*. Scale bar equals 2 cm.

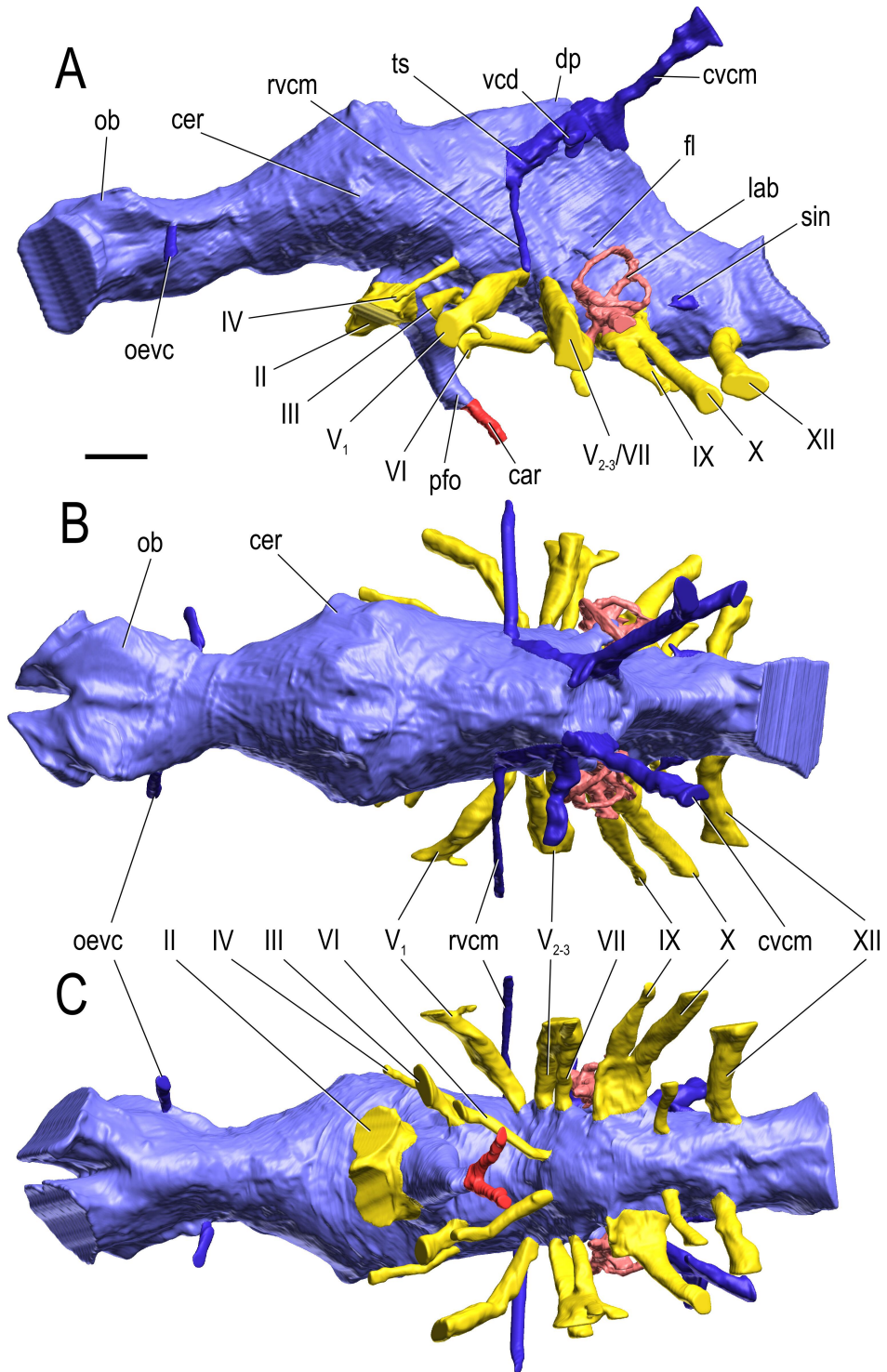


FIG. 6.10. Cranial endocast, endosseous labyrinth, and some endocranial vascular structures of the theropod dinosaur, *Tyrannosaurus rex* (AMNH 5117), derived from surface renderings of CT scan data. **A**, left lateral view. **B**, dorsal view. **C**, ventral view. Color scheme: cranial endocast, *blue*; endosseous labyrinth, *pink*; nerve canals (most of which also transmit veins), *yellow*; smaller venous canals, *dark blue*; arterial canals, *red*. Scale bar equals 2 cm.

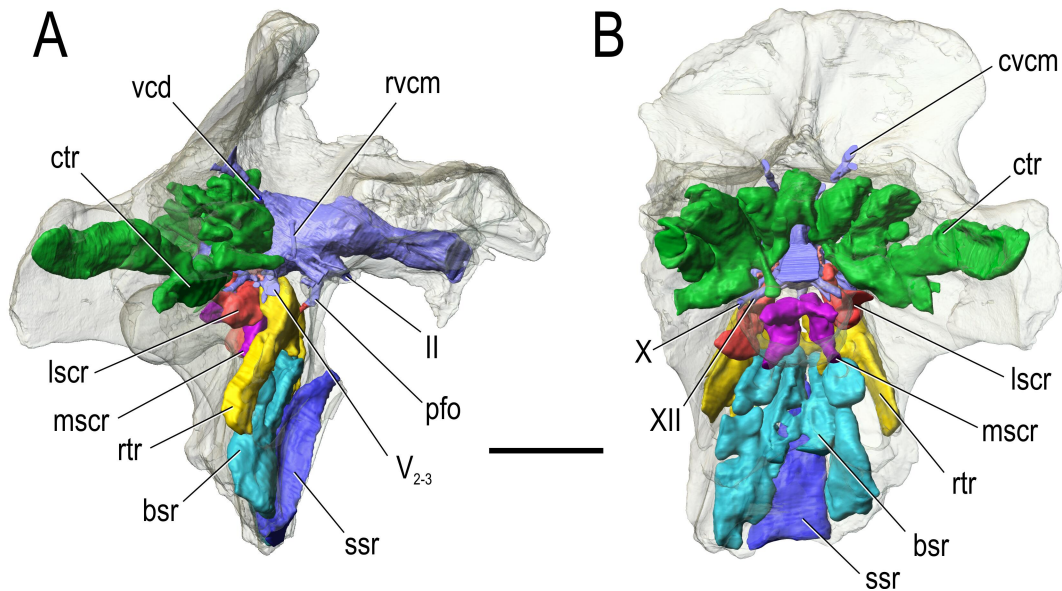


FIG. 6.11. Pneumatic sinuses and cranial endocast within the semitransparent bony braincase of the theropod dinosaur, *Tyrannosaurus rex* (AMNH 5117), derived from surface renderings of CT scan data. **A**, right lateral view. **B**, caudal view. Scale bar equals 10 cm.

H. Endo · R. Frey (Eds.)

Anatomical Imaging

Towards a New Morphology

 Springer

HIDEKI ENDO, Ph.D.
Professor, The University Museum, The University of Tokyo
7-3-1 Hongo, Bunkyo-ku, Tokyo 113-0033, Japan

ROLAND FREY, Ph.D.
Research Group: Reproduction Management, Leibniz Institute for Zoo and Wildlife
Research (IZW)
Alfred-Kowalke-Strasse 17, 10315 Berlin, Germany

ISBN 978-4-431-76932-3 Springer Tokyo Berlin Heidelberg New York
eISBN 978-4-431-76933-0

Library of Congress Control Number: 2008928682

Printed on acid-free paper

© Springer 2008

Printed in Japan

This work is subject to copyright. All rights are reserved, whether the whole or part of the material is concerned, specifically the rights of translation, reprinting, reuse of illustrations, recitation, broadcasting, reproduction on microfilms or in other ways, and storage in data banks.

The use of registered names, trademarks, etc. in this publication does not imply, even in the absence of a specific statement, that such names are exempt from the relevant protective laws and regulations and therefore free for general use.

Springer is a part of Springer Science+Business Media
springer.com

Typesetting: SNP Best-set Typesetter Ltd., Hong Kong
Printing and binding: Nikkei Printing, Japan